

Chapter 2

Atmospheric Radiative Transfer

The interaction between atmospheric matter and solar and terrestrial radiation plays a leading role for life conditions at the Earth's surface:

- stratospheric ozone filters the solar ultraviolet radiation;
- the absorption by a few gas-phase species (e.g. water, methane or carbon dioxide) of the terrestrial radiation defines the so-called *greenhouse effect*, which results in a surface temperature greater than 273 K (otherwise, the Earth would be a “white planet”);
- more generally, the state of the atmosphere is determined by its energy budget, comprising the radiative fluxes (solar and terrestrial radiation) and the latent and sensible heat fluxes.¹

The radiative properties and the concentrations of the atmospheric *trace species* determine the general behavior of the atmosphere. For example, a few species, emitted by anthropogenic activities, play a decisive role by increasing the greenhouse effect or by decreasing the filtration of ultraviolet radiation (by taking part in the consumption of stratospheric ozone).

At first glance, the energy budget of the Earth/atmosphere system should not be perturbed by anthropogenic activities (Table 2.1). The Earth and the atmosphere absorb 235 W m^{-2} of solar radiation, to be compared with 0.087 W m^{-2} of internal energy flux (geothermy) and with the energy directly related to anthropogenic activities, 0.025 W m^{-2} . However, there is an indirect anthropogenic contribution to this energy budget, which is deeply related to pollution. Emission of greenhouse gases will indeed imply much stronger effects: the radiative forcing due to greenhouse gases since pre-industrial times is estimated to be about 2.5 W m^{-2} , which means that the scaling factor (for the direct contribution) is 100!

This chapter is organized as follows. A primer for radiative transfer is given in Sect. 2.1, with the description of radiative emission, absorption and scattering. Section 2.2 illustrates the application to the atmosphere, with a focus on the greenhouse effect. The main sources of uncertainties, namely the role of clouds and aerosols,

¹Latent heat is associated to the condensation of water vapor, an exothermic process; the sensible heat is associated to turbulence.

Table 2.1 Energy fluxes for the Earth/atmosphere system. Source: [25]

Solar energy absorbed by the Earth and the atmosphere	235 W m^{-2}
Internal energy flux (geothermy)	0.087 W m^{-2}
Anthropogenic energy production	
average	0.025 W m^{-2}
urban area	$\simeq 50 \text{ W m}^{-2}$
Radiative forcing due to greenhouse gases	$\simeq 2.5 \text{ W m}^{-2}$
since the preindustrial times	

are also detailed. The link between particulate pollution and visibility reduction is briefly presented at the end of this chapter.

2.1 Primer for Radiative Transfer

The atmosphere filters the energy received from the Sun and from the Earth. Radiative transfer describes the interaction between radiation and matter (gases, aerosols, cloud droplets). The three key processes to be taken into account are:

- *emission*;
- *absorption* of an incident radiation by the atmospheric matter (which corresponds to a decrease of the radiative energy in the incident direction);
- *scattering* of an incident radiation by the atmospheric matter (which corresponds to a redistribution of the radiative energy in all the directions).

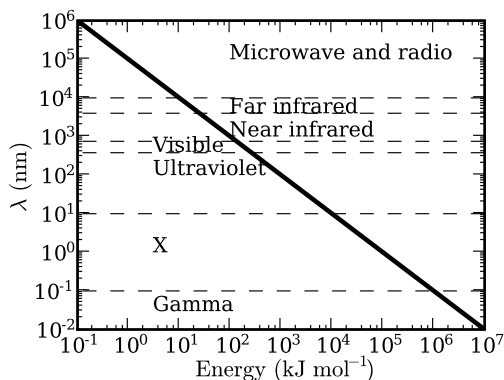
2.1.1 Definitions

2.1.1.1 Radiation

There are two possible viewpoints for describing electromagnetic radiations. A radiation is composed of particles, the so-called *photons*. Similarly, it can be viewed as a wave propagating at the speed of light ($c \simeq 3 \times 10^8 \text{ m s}^{-1}$ in a vacuum, a similar value in air). It is then characterized by its frequency ν (in s^{-1} or in hertz) or, equivalently, by its wavelength $\lambda = c/\nu$ (usually expressed in nm or in μm).

As shown in Fig. 2.1, the radiation spectrum can be divided into wavelength regions: γ -ray region ($\lambda \leq 0.1 \text{ nm}$), X-ray radiation ($0.1 \text{ nm} \leq \lambda \leq 10 \text{ nm}$), ultra-violet radiation ($10 \text{ nm} \leq \lambda \leq 380 \text{ nm}$), visible radiation (“light”, from blue to red: $380 \text{ nm} \leq \lambda \leq 750 \text{ nm}$), infrared radiation ($750 \text{ nm} \leq \lambda \leq 10 \mu\text{m}$), microwave region, etc.

Fig. 2.1 Decomposition of the electromagnetic spectrum. *Abscissa*: energy (in kJ mol^{-1}); *ordinate*: wavelength (in nm)



2.1.1.2 Solid Angle

The concept of *solid angle* is used for quantifying the solar radiation received by a surface. Let σ be a surface element on a sphere of radius r centered at point O . A solid angle Ω is then defined as the ratio of σ to the square of r : $\Omega = \sigma/r^2$.

In spherical coordinates, the differential surface element $d\sigma$ is generated by the variations of the *zenithal* angle $d\theta$ and of the *azimuthal* angle $d\phi$ (Fig. 2.2). The differential solid angle is then given by

$$d\Omega = \frac{d\sigma}{r^2}. \quad (2.1)$$

Since $d\sigma = r \sin \theta d\phi \times r d\theta$, this yields

$$d\Omega = \sin \theta d\phi d\theta. \quad (2.2)$$

A solid angle is measured in *steradian* (sr). For a sphere, as $\theta \in [0, \pi]$ and $\phi \in [0, 2\pi]$, we obtain upon integration $\Omega = 4\pi$.

2.1.1.3 Radiance and Irradiance

We consider a differential surface area dA (Fig. 2.2). Let dE_λ be the radiative energy (expressed in joules) intercepted by dA for incident photons of wavelength in $[\lambda, \lambda + d\lambda]$, during a time interval dt , in the solid angle $d\Omega$. The *monochromatic radiance* is defined as the energy that is propagated through the surface dS generated by dA in a direction perpendicular to the incident direction ($dS = \cos \theta \times dA$), namely

$$dI_\lambda = \frac{dE_\lambda}{dS d\lambda dt d\Omega}. \quad (2.3)$$

The radiance is usually expressed in $\text{W m}^{-2} \text{nm}^{-1} \text{sr}^{-1}$ (with $1 \text{ W} = 1 \text{ J s}^{-1}$).

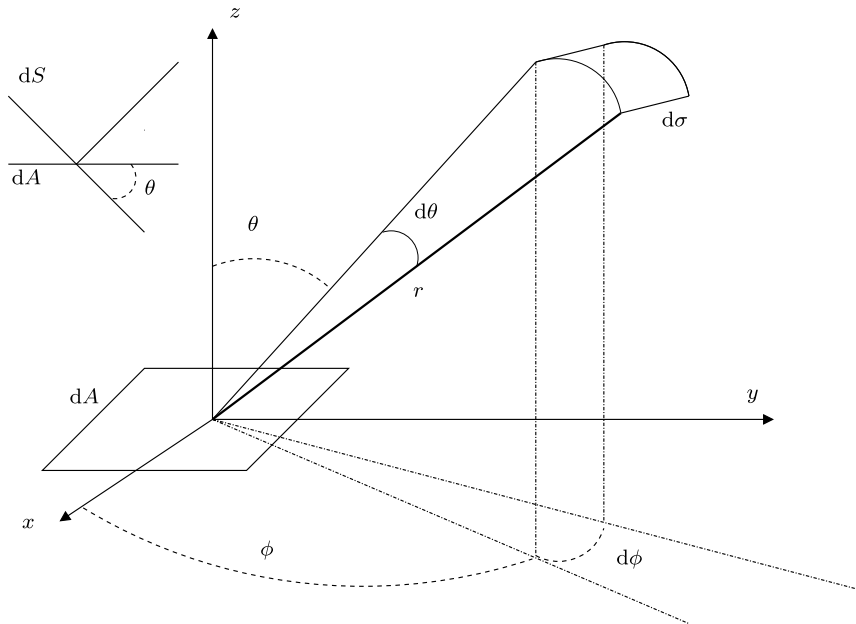


Fig. 2.2 Definition of a solid angle. In the *left part* of the figure, the surface elements dA and dS are represented by their projection in a vertical plane

Monochromatic irradiance is defined as the component of the monochromatic radiance that is normal to dA , upon integration over the whole solid angle (the normal direction is given by the vertical axis in Fig. 2.2),

$$F_{\lambda} = \int_{\Omega} \cos \theta I_{\lambda} d\Omega. \quad (2.4)$$

Upon integration over all the wavelengths, the *irradiance* is defined by $F = \int_{\lambda} F_{\lambda} d\lambda$. It is expressed as a (received) power per unit area of surface (in W m^{-2}).

2.1.2 Energy Transitions

Quantum mechanics describes the energy levels of a given molecule. The key point is that the energy levels are given by a *discrete* sequence, let us say $(E_n)_n$, specific of the *spectroscopic properties* of the molecule.

The simplest illustration is detailed in Exercise 2.1, with the case of a particle supposed to be “trapped in a well”.

Exercise 2.1 (Discrete Energy Levels) Consider a particle “trapped in a well” (the well is actually defined by an energy potential). For convenience, we suppose that

the well corresponds to a one-dimensional interval, let us say $[0, 1]$. Let x be the spatial variable.

The particle location is described by a *probability density function*, $p(x)$, which can be computed from the wavefunction $f(x)$ as $p(x) = |f(x)|^2$. The wavefunction is governed by the Schrödinger equation

$$-\frac{h^2}{2m} \frac{d^2 f}{dx^2} + V(x)f = Ef,$$

where m is the particle mass, $V(x)$ is the energy potential that defines the well, E corresponds to the particle energy and $h = 6.63 \times 10^{-34}$ J s is Planck's constant.

The particle motion is free inside the well ($V = 0$) but the particle is “trapped” (its probability density function is null at the boundaries). Calculate the possible levels of energy (E).

Solution:

The governing equation for f is

$$\frac{d^2 f}{dx^2} = -\frac{2mE}{h^2} f, \quad f(0) = f(1) = 0.$$

The solutions are in the form $f(x) \sim \sin(\sqrt{\frac{2mE}{h^2}}x)$ where $\sqrt{\frac{2mE}{h^2}} = n\pi$ with n a positive integer. This results in a discrete spectrum of possible values for the energy level, $E_n = n^2 \frac{h^2}{2m} \pi^2$.

Consider a molecule with a given energy level, let us say E_1 . The emission of a photon by this molecule corresponds to a transition from E_1 to a lower energy level, let us say $E_2 < E_1$. On the opposite, the absorption of a photon by this molecule implies the transition from E_1 to a higher energy level, let us say $E_2 > E_1$. The wavelength of the photon is fixed by the energy transition. Planck's law (Fig. 2.3) states that

$$\Delta E = h\nu = \frac{hc}{\lambda}. \quad (2.5)$$

A photon can therefore be absorbed or emitted only if its wavelength corresponds to a possible transition. As a result, for a given molecule, absorption and emission are possible only in specific parts of the radiation spectrum (determined by the spectroscopic properties of the molecule).

If λ has a small value, the energy gap is large: the shortwave radiations (e.g. ultra-violet radiation) are the most energy-containing ones (Fig. 2.1). On the other hand, if the wavelength has a large value, the energy gap is low: the longwave radiations (e.g. infrared radiation) do not contain a lot of radiative energy.

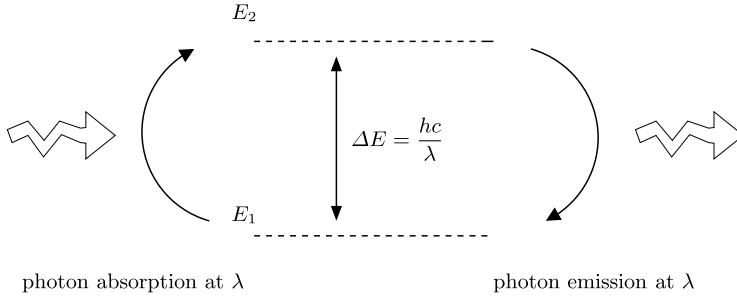


Fig. 2.3 Emission and absorption of a photon: transition between two energy levels E_1 and E_2 ($E_1 < E_2$). The wavelength is given by Planck's law, $\lambda = hc/(E_2 - E_1)$

2.1.3 Emissions

2.1.3.1 Blackbody Emission

Planck's Distribution The radiative energy emitted by a "body" at equilibrium depends on its temperature. Intuitively, it is expected that the higher the temperature is, the higher the emission is.

The maximum of radiative energy that can be emitted per unit area of surface and per time unit defines the so-called *blackbody emission*. For a body at temperature T , the maximum of emitted radiance at wavelength λ is given by the so-called Planck distribution,

$$B_\lambda(T) = \frac{2hc^2}{\lambda^5} \frac{1}{\exp\left(\frac{hc}{\lambda k_B T}\right) - 1}, \quad (2.6)$$

where $k_B = 1.38 \times 10^{-23} \text{ J K}^{-1}$ is Boltzmann's constant. The unit is $\text{W m}^{-2} \text{ nm}^{-1}$.

Remark 2.1.1 (Shape of Planck's Distribution) Let us try to justify the qualitative shape of Planck's distribution (following A. Einstein).

Consider a blackbody, defined as a substance that absorbs all incident radiation. The blackbody is supposed to be inside a box, such that the walls do not emit nor absorb radiation. The reflection on the walls are therefore supposed to be perfect. Thus, the blackbody receives an incident radiation, I , that is exactly the emitted radiation.

Let $E_1 < E_2$ be two energy levels of the blackbody. At equilibrium, the probability of having E_i ($i = 1, 2$) is given by the Maxwell-Boltzmann distribution and is equal to $\exp(-E_i/k_B T)$, up to a normalization factor.

The probability $P_{1 \rightarrow 2}$ that the absorption of radiation leads to a transition from E_1 to a higher value E_2 is proportional to the number of molecules at state E_1 , namely

$$P_{1 \rightarrow 2} = \alpha I \exp\left(-\frac{E_1}{k_B T}\right) \quad (2.7)$$

with α a multiplying factor.

The transition from E_2 to a lower value E_1 is driven by two processes: first, the spontaneous emission of a photon and, second, the emission induced by the absorption of the incident radiation, I . The transition probability $P_{2 \rightarrow 1}$ is therefore composed of two terms: the first one is proportional to the number of molecules at state E_2 while the second one is proportional to I . Thus,

$$P_{2 \rightarrow 1} = \underbrace{\beta I \exp\left(\frac{-E_2}{k_B T}\right)}_{\text{induced emission}} + \underbrace{\gamma \exp\left(\frac{-E_2}{k_B T}\right)}_{\text{spontaneous emission}}, \quad (2.8)$$

with β and γ two multiplying factors.

At equilibrium, $P_{1 \rightarrow 2} = P_{2 \rightarrow 1}$, so that the number of molecules at a given energy level is constant. The incident radiation is exactly the emitted radiation and satisfies

$$I = \frac{\gamma}{\alpha \exp\left(-\frac{\Delta E}{k_B T}\right) - \beta}, \quad (2.9)$$

with $\Delta E = E_2 - E_1$, connected to the wavelength λ by $\Delta E = hc/\lambda$.

This justifies Planck's law, (2.6), if $\alpha = \beta$, namely if the probability of absorption is equal to the probability of induced emission.

Wien's Displacement Law Planck's distribution is an increasing function with respect to temperature (T) and is a concave function of the wavelength (λ). At fixed T , the wavelength of the maximum is given by $\partial B_\lambda / \partial \lambda = 0$. This yields (expressed in nm)

$$\lambda_{\max} \simeq \frac{2898 \times 10^3}{T}. \quad (2.10)$$

λ_{\max} is inversely proportional to the temperature. This is the so-called Wien's displacement law: a warm body emits shortwave radiations, corresponding to energy-containing radiations.

Stefan-Boltzmann Law Upon integration over the entire wavelength domain, the total emitted radiance of a blackbody at temperature T is

$$B(T) = \int_0^{+\infty} B_\lambda(T) d\lambda = \sigma T^4. \quad (2.11)$$

The unit is W m^{-2} .

Admitting that $\int_0^\infty v^3 dv / (e^v - 1) = \pi^4/15$, the Stefan-Boltzmann constant is² $\sigma = 2\pi^5 k_B^4 / (15c^2 h^3)$, namely $\sigma = 5.67 \times 10^{-8} \text{ W m}^{-2} \text{ K}^{-4}$. As expected, the radiative energy emitted by a blackbody is an increasing function of the temperature (proportional to the fourth power of the temperature).

²The notation could be misleading with respect to that of a differential area used for solid angles.

Table 2.2 Typical values of the emissivity in the infrared region, for different surface types. Source: [67]

Surface	ϵ_{IR}	Surface	ϵ_{IR}
Sea	0.95–1	Grass	0.90–0.95
Fresh snow	0.99	Desert	0.85–0.90
“Old” snow	0.80	Forest	0.95
Liquid water clouds	0.25–1	Concrete	0.70–0.90
Cirrus	0.10–0.90	Urban	0.85

2.1.3.2 Emissivity

A realistic medium is not a blackbody. The radiative energy that is actually emitted by a medium at temperature T , for a given wavelength λ , is

$$E_\lambda(T) = \epsilon_\lambda(T) B_\lambda(T), \quad (2.12)$$

where $\epsilon_\lambda(T)$ is the so-called *emissivity* at wavelength λ and at temperature T . By definition, $\epsilon_\lambda \leq 1$ (unitless).

For example, in the case of infrared radiation, the radiative behavior of fresh snow (the “whitest” snow) is similar to a blackbody,³ with $\epsilon_\lambda \simeq 1$ (Table 2.2). On the opposite, the urban environment has a low emissivity, which will strongly impact the urban climate (Sect. 3.6).

2.1.3.3 Application to the Earth and to the Sun

The Sun can be considered as a blackbody with a temperature of 5800 K. Applying Wien’s law justifies that the Sun’s emission peaks in the visible region (maximum at 500 nm). The Earth can be considered as a blackbody at 288 K. The maximum is then in the infrared region (10 μm).

Upon a direct application of the Stefan-Boltzmann law, the Sun emits about 20^4 as much as the Earth ($5800/288 \simeq 20$).

The key point is that both emitted radiation spectra can be *split* (Fig. 2.4). The atmosphere will have a different behavior with respect to the solar and terrestrial radiation: in a first approximation, the infrared terrestrial radiation is absorbed while the atmosphere is transparent to the solar visible radiation.

2.1.4 Absorption

2.1.4.1 Beer-Lambert Law

A fraction of the incident radiation is absorbed along the path of propagation in a medium (here the atmosphere). The Beer-Lambert law (also referred to as the Beer-

³The terminology has nothing to do with colors!

Fig. 2.4 Normalized emission spectrum for the Earth (blackbody at $T = 288$ K) and for the Sun (blackbody at $T = 5800$ K)

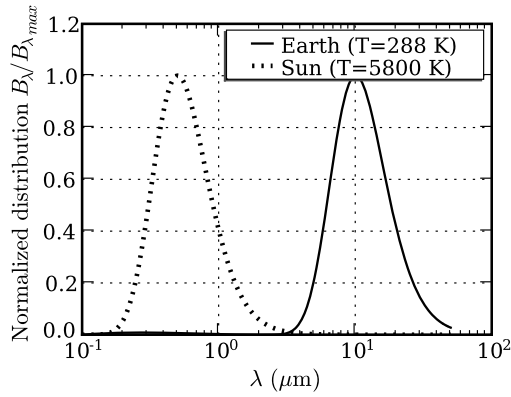
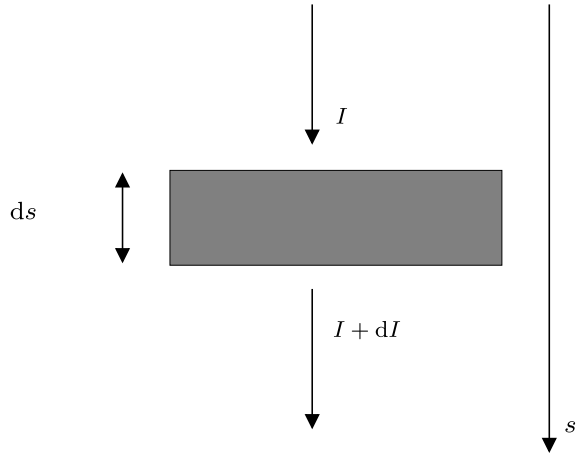


Fig. 2.5 Absorption of an incident radiation traversing a medium (*gray box*)



Lambert-Bouguer law) governs the reduction in the radiation intensity I_λ at wavelength λ (Fig. 2.5). If s stands for the medium thickness (oriented in the direction of propagation), the evolution of the radiation intensity is

$$\frac{dI_\lambda}{ds} = -a_\lambda(s)I_\lambda, \quad (2.13)$$

where $a_\lambda(s)$ is the absorption coefficient at wavelength λ (depending on the medium). The unit of a_λ is, for instance, m^{-1} or cm^{-1} . Assuming that the medium is homogeneous, then a_λ has a constant value and

$$I_\lambda(s) = I_\lambda(0) \times \exp(-sa_\lambda). \quad (2.14)$$

Consider a medium composed of p absorbing species, with densities n_i ($i = 1, \dots, p$), expressed in molecule cm^{-3} . The absorbing coefficient is then obtained by summing over all species. For a given species, the contribution depends on the density and on the so-called *absorption cross section* (the effective cross section

resulting in absorption), $\sigma_i^a(\lambda, s)$, usually expressed in cm^2 :

$$a_\lambda(s) = \sum_{i=1}^p n_i(s) \sigma_i^a(\lambda, s). \quad (2.15)$$

A way to define the absorption cross section is to consider an incident flux of energy per surface, F (in W cm^{-2}). The resulting absorbed energy is then $F_a = \sigma_a \times F$ (expressed in W).

Another classical concept is the so-called *optical depth* τ_λ (unitless), defined for a monochromatic radiation by

$$d\tau_\lambda = a_\lambda(s) ds. \quad (2.16)$$

Rewriting the Beer-Lambert law yields

$$\frac{dI_\lambda}{d\tau_\lambda} = -I_\lambda. \quad (2.17)$$

2.1.4.2 Kirchhoff's Law

For a given wavelength λ , the *absorptivity* A_λ is defined as the fraction of the incident radiation that is absorbed by the medium. Kirchhoff's law (1859) connects the absorptivity and the emissivity of a medium at thermodynamic equilibrium, namely

$$\epsilon_\lambda = A_\lambda. \quad (2.18)$$

The absorption properties of a medium are therefore directly related to its emission properties.

Note that A_λ can be derived from a_λ . For a medium supposed to be homogeneous, with a thickness Δz (typically a cloud), with an absorbing coefficient a_λ , the ratio of the absorbed intensity to the incident intensity is $A_\lambda = 1 - \exp(-a_\lambda \Delta z)$.

At thermodynamic equilibrium, when taking into account absorption and emission, the evolution of the intensity is then

$$\frac{dI_\lambda}{ds} = a_\lambda(s)(B_\lambda(T) - I_\lambda). \quad (2.19)$$

2.1.4.3 Spectral Line Broadening

For a given energy transition ΔE , Planck's law describes only monochromatic absorption or emission, with a unique wavelength λ_0 , given by $|\Delta E| = hc/\lambda_0$. This defines the so-called *spectral lines*. In practice, monochromatic radiations are not observed. As shown by the absorption spectrum for a few species (Sect. 2.2), there is a *broadening* of the wavelengths, mainly related to two effects.

Doppler Broadening For moving molecules, the *Doppler effect* implies that the emission and absorption wavelengths are broadened. This is usually described by the so-called Doppler profile, centered at λ_0 , given by a Gaussian distribution with respect to the frequency $\nu = c/\lambda$,

$$f_D(\nu) = \frac{S_D}{\alpha_D} \sqrt{\frac{\ln 2}{\pi}} \exp\left(-\frac{(\nu - \nu_0)^2}{\alpha_D^2} \ln 2\right), \quad (2.20)$$

where α_D and S_D stand for the half width of the line and the line strength, respectively. The half width of the line is related to the velocity of the molecule in the direction of the incident radiation, and is proportional to \sqrt{T} .

This shape is derived from the probability density function of the velocity, given by the Maxwell distribution

$$P(v) = \sqrt{\frac{m}{2\pi k_B T}} \exp\left(-\frac{mv^2}{2k_B T}\right) \quad (2.21)$$

with m the molecule mass. The Doppler effect states that the frequency ν appears shifted as seen by a stationary observer to the frequency $\tilde{\nu} = \nu(1 \pm v/c)$.

Pressure Broadening (Lorentz Effect) The collisions between the molecules contribute to broaden the lines. The distribution function is then

$$f_L(\nu) = \frac{S_L}{\pi} \frac{\alpha_L}{(\nu - \nu_0)^2 + \alpha_L^2} \quad (2.22)$$

where α_L and S_L stand for the width and the strength of the line, respectively. The width is related to the collision frequency and is proportional to the product of the molecule density, n , by the velocity (proportional to \sqrt{T}). With the ideal gas law, $n \propto P/T$ (P is the pressure), and thus $\alpha_L \propto P/\sqrt{T}$.

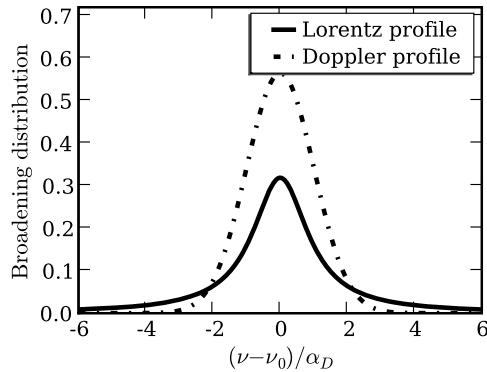
The Lorentz effect is a decreasing function of altitude. For a hydrostatic atmosphere (Chap. 1), supposed to be adiabatic (Chap. 3), the vertical profiles of pressure and of temperature are indeed $P(z) \simeq P_0 \exp(-z/H)$ and $T(z) \simeq T_0 - \Gamma z$.

The typical shape of the Doppler and Lorentz profiles is shown in Fig. 2.6. Up to 40 kilometers, the Lorentz effect is the dominant effect (due to high densities), then the Doppler effect and, finally, the joint impact of both effects (described by the so-called *Voigt profile*).

2.1.5 Scattering

Let us consider a gaseous molecule or a particle (aerosol or cloud drop), with a characteristic size. The incident radiation is also *scattered* in all directions. The shape of the scattered intensity strongly depends on the characteristic size.

Fig. 2.6 Normalized distribution functions for the Lorentz and Doppler effects



2.1.5.1 Scattering Regimes

The scattering of the incident electromagnetic wave by a gas-phase molecule or by a particle mainly depends on the comparison between the wavelength (λ) and the characteristic size (d). We recall that $d \simeq 0.1$ nm for a gas-phase molecule, $d \in [10 \text{ nm}, 10 \mu\text{m}]$ for an aerosol and $d \in [10, 100] \mu\text{m}$ for a liquid water drop (Chap. 1). The wide range covered by the body size will induce different behaviors.

Three scattering regimes are usually distinguished: the Rayleigh scattering (typically for gases), the scattering represented by the optical geometry's laws (typically for liquid water drops) and the so-called Mie scattering (for aerosols).

Rayleigh Scattering If $d \ll \lambda$ (the case for gases), the electromagnetic field can be assumed to be homogeneous at the level of the scattering body. This defines the so-called *Rayleigh scattering* (also referred to as *molecular scattering*).

The scattered intensity in a direction with an angle θ to the incident direction, at the distance r from the scattering body (see Fig. 2.7), for a media of mass concentration C , composed of spheres of diameter d and of density ρ , is then given by ([89])

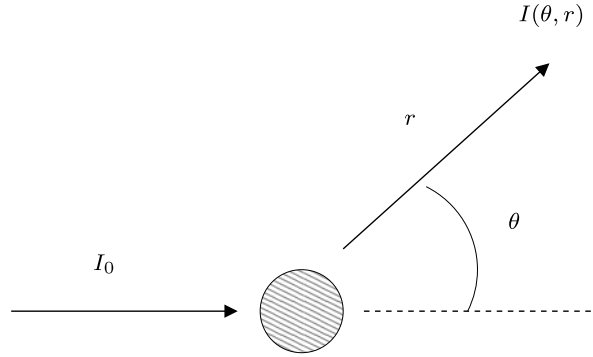
$$I(\theta, r) = I_0 \frac{8\pi^4}{r^2 \lambda^4} \frac{\rho^2 d^6}{C^2} \left(\frac{m^2 - 1}{m^2 + 2} \right)^2 (1 + \cos^2 \theta). \quad (2.23)$$

The incident intensity is I_0 . m is the complex refractive index, specific to the scattered body: it is defined as the ratio of the speed of light in the vacuum to that in the body, and depends on the chemical composition for aerosols (e.g. $m = 1.34$ for water at $\lambda = 450$ nm, Table 2.3).

This formula is inversely proportional to λ^4 : scattering is therefore much stronger for the shortwave radiations (Remark 2.1.2 devoted to the sky color). As a result, the terrestrial longwave radiations are weakly scattered.

Note that the Rayleigh scattering is an increasing function of the size (d) and is a decreasing function of the distance (r). Moreover, Rayleigh scattering is symmetric between the backward and forward directions: $I(\theta, r) = I(\pi - \theta, r)$.

Fig. 2.7 Scattering of an incident radiation (I_0)



Optical Geometry If $d \gg \lambda$ (this is the case of liquid water drops with respect to the solar radiation), the laws of optical geometry can be applied, leading to the understanding of many physical phenomena (e.g. rainbow formation). The scattering weakly depends on the wavelength.

Mie Scattering If $d \simeq \lambda$ (the case for most of atmospheric aerosols), the simplifications used above are no longer valid. A detailed calculation of the interaction between the electromagnetic field and the scattering body is required: this is given by the *Mie theory*.

The intensity of the scattered radiation in the direction with an angle θ to the incident direction, at a distance r , is ([89])

$$I(\theta, r) = I_0 \frac{\lambda^2(i_1 + i_2)}{4\pi^2 r^2}, \quad (2.24)$$

where i_1 and i_2 are the intensity Mie parameters, given as complicated functions of d/λ , θ and m . The parameters i_1 and i_2 are characterized by a set of *maxima* as a function of the angle θ . Note that the forward fraction of the scattering intensity is dominant (Fig. 2.8).

Remark 2.1.2 (Sky Color) In a simplified approach, the intensity scattered by aerosols can be parameterized as a function proportional to $\lambda^{-1.3}$. As a result, the scattering does not filter specific wavelengths, which explains why polluted skies (with high concentrations of particulate matter) are gray (Sect. 2.2.5).

On the opposite, for a “clean” sky (sometimes referred to as “Rayleigh sky”), Rayleigh scattering can be applied. The scattering bodies are gas-phase molecules, such as N_2 and O_2 , whose characteristic size is about one angström (0.1 nm). The solar radiation is mainly in the visible region (the X-rays and the ultraviolet radiation have been filtered in the ionosphere and in the stratosphere, respectively). The dependence in λ^{-4} peaks the scattered intensity in the smallest wavelengths (those corresponding to the blue color).

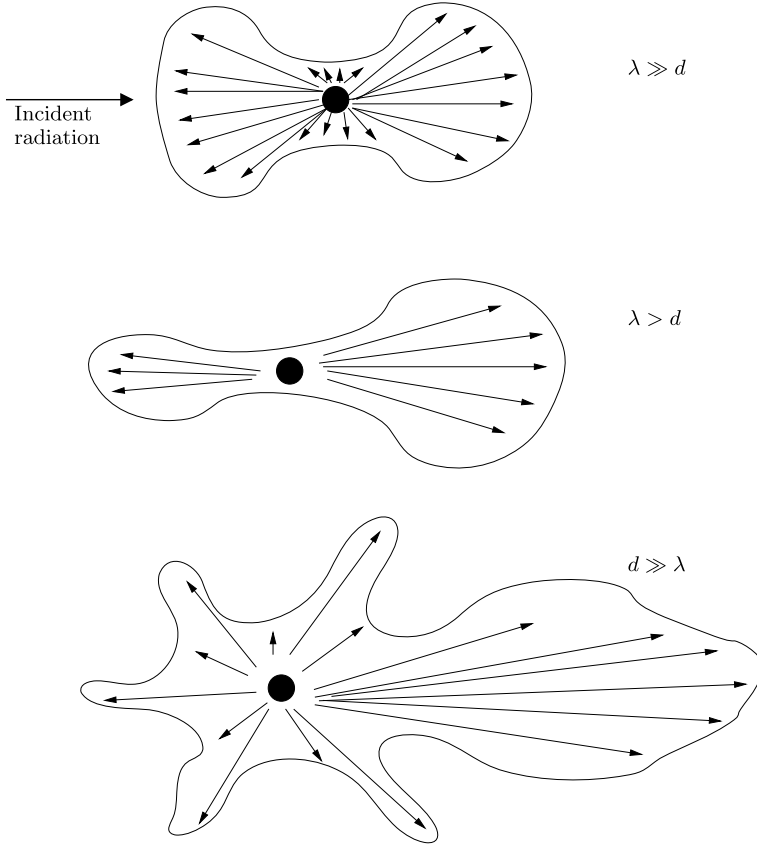


Fig. 2.8 Scattering of an incident radiation of wavelength λ by an aerosol (gray sphere) of diameter d . The size of the vectors originating from the aerosol is proportional to the scattered intensity in the vector direction

2.1.5.2 Modeling of Scattering

Modeling the scattering requires us to describe the intensity as a function of not only the medium thickness (s) but also of the solid angle $\Omega = (\theta, \phi)$.

The evolution of the intensity is given by

$$\frac{dI_\lambda}{ds} = -d_\lambda(s)I_\lambda + \frac{d_\lambda}{4\pi} \int P(\Omega, \Omega') I_\lambda(\Omega') d\Omega'. \quad (2.25)$$

The first term, similar to the Beer-Lambert law, corresponds to an extinction of the incident radiation. The scattering coefficient $d_\lambda(s)$ (for instance expressed in cm^{-1})

is given, similar to absorption, by

$$d_\lambda(s) = \sum_{i=1}^p n_i(s) \sigma_i^d(\lambda, s), \quad (2.26)$$

with $\sigma_i^d(\lambda, s)$ the scattering cross section for species i (expressed e.g. in cm^{-2}). Similar to absorption, the scattering cross section can be defined as the fraction of the incident flux of energy that is scattered. Let F be the incident flux of energy per surface (in W cm^{-2}). The scattered energy, F_d (in W), is then given by

$$F_d = \sigma_d \times F. \quad (2.27)$$

The second source term in (2.25) corresponds to the scattering in all the directions. The scattering probability density function, $P(\Omega, \Omega')$, describes the scattering from the solid angle Ω to the solid angle Ω' . It satisfies

$$\frac{1}{4\pi} \int P(\Omega, \Omega') d\Omega' = 1. \quad (2.28)$$

2.1.6 Radiative Transfer Equation

The three processes (emission, absorption and scattering) are actually coupled. The radiative transfer equation reads

$$\frac{dI_\lambda}{ds} = -(a_\lambda(s) + d_\lambda(s))I_\lambda(s) + a_\lambda(s)B_\lambda(T) + \frac{d_\lambda}{4\pi} \int P(\Omega, \Omega') I_\lambda(\Omega') d\Omega'. \quad (2.29)$$

The sum $a_\lambda + d_\lambda$ defines the *extinction coefficient*, usually written as b_λ^{ext} .

The optical depth determines the opacity of the medium and is defined, similar to (2.16), by

$$d\tau_\lambda = (a_\lambda(s) + d_\lambda(s))ds. \quad (2.30)$$

Thus

$$\frac{dI_\lambda(\tau)}{d\tau} = -I_\lambda(\tau) + \omega_a B_\lambda(T(\tau)) + \frac{\omega_d}{4\pi} \int P(\Omega, \Omega') I_\lambda(\Omega') d\Omega', \quad (2.31)$$

where $\omega_a = a_\lambda/(a_\lambda + d_\lambda)$ and $\omega_d = d_\lambda/(a_\lambda + d_\lambda)$ are the absorption and scattering albedos, respectively.

We investigate two simplified cases: the case of infrared radiation (only absorption and emission are taken into account) and the case of visible radiation (only scattering is described).

2.1.6.1 Infrared Radiation

Scattering can be neglected for the infrared radiation. Moreover, the temperature T is a function of the altitude: we write $T(\tau)$ with τ an increasing function of the altitude (the terrestrial radiation propagates from the bottom to the top of the atmosphere).

Integrating (2.31) yields

$$I_\lambda(\tau) = I_\lambda(0)e^{-\tau} + \int_0^\tau B_\lambda(T(\tau'))e^{(\tau'-\tau)} d\tau'. \quad (2.32)$$

The first term is a pure extinction term while the second term describes the emission from the atmosphere. $I_\lambda(0)$ is the emitted radiation at the Earth's surface.

2.1.6.2 Visible Radiation

For the visible region of the electromagnetic spectrum, we can neglect both absorption and emission in the atmosphere. Thus,

$$\frac{dI_\lambda(\tau)}{d\tau} = -I_\lambda(\tau) + \frac{1}{4\pi} \int P(\Omega, \Omega') I_\lambda(\Omega') d\Omega'. \quad (2.33)$$

In this case, the optical depth, τ , is a decreasing function of the altitude (the radiation propagates from the top to the bottom of the atmosphere). The boundary condition $I_\lambda(0)$ corresponds to the solar radiation received at the top of the atmosphere.

There does not exist any analytical solution in the general case. Solving this equation can be performed with the *method of successive orders*. The solution is built by solving successively the systems

$$\frac{dI_\lambda^{n+1}(\tau)}{d\tau} = -I_\lambda^{n+1}(\tau) + \frac{1}{4\pi} \int P(\Omega, \Omega') I_\lambda^n(\Omega') d\Omega'. \quad (2.34)$$

Scattering is then applied to the radiation computed in the previous iteration. We can then apply a superposition approach since the radiative transfer equation is linear, yielding $I_\lambda = \sum_{n=0}^{\infty} I_\lambda^n$.

2.1.7 Additional Facts for Aerosols

The extinction properties of a particle are determined by its *extinction efficiency*, defined as the ratio of the scattering cross section to the interception surface. For a particle of diameter d , the interception surface is $A = \pi(d/2)^2$. The extinction comprises a part associated to absorption and a part associated to scattering, namely

$$Q_\lambda^{ext} = Q_\lambda^a + Q_\lambda^d = \frac{\sigma_\lambda^a + \sigma_\lambda^d}{\pi(d/2)^2}. \quad (2.35)$$

Table 2.3 Typical values of the complex refractive index ($n_\lambda + jk_\lambda$), for a few aerosol types. The wavelength is $\lambda = 450$ nm, corresponding to visible radiation. Source: [53]

Aerosol type	n_λ	k_λ
Water	1.34	0.
Ammonium	1.53	-5×10^{-3}
Sulfate	1.43	0.
Sea salt	1.5	0.
Soot	1.75	-0.45
Mineral aerosol	1.53	-8.5×10^{-3}
Organic aerosol	1.53	-8.5×10^{-3}

The absorption and scattering efficiencies, Q_λ^a and Q_λ^d respectively, are functions of

- the *size parameter*

$$\alpha_\lambda = \frac{\pi d}{\lambda}, \quad (2.36)$$

with d the particle diameter (the particle is supposed to be a sphere);

- the properties of the medium defined by the particle (due to its chemical composition), described by its *complex refractive index*

$$m_\lambda = n_\lambda + jk_\lambda, \quad j^2 = -1. \quad (2.37)$$

The real part n_λ is related to scattering while the imaginary part k_λ is related to absorption.

Actually, m_λ is normalized with respect to the “ambient” medium (here, air, whose refractive index is about 1 for visible radiation).

The refractive index in the visible region of the electromagnetic spectrum is given in Table 2.3 for different particle types (with different chemical composition). Note that soot (*elemental* or *black carbon*) is characterized by a strong absorption.

The extinction coefficient for a particle can be deduced from the extinction efficiency. For a particle density n (expressed in number of particles per volume of air), we obtain

$$b_\lambda^{ext} = \sigma_\lambda^{ext} \times n = \frac{\pi d^2}{4} Q_\lambda^{ext} n. \quad (2.38)$$

The extinction efficiency is a function of the refractive index (m_λ) and of the size parameter (α_λ). For large values of the size parameter ($d/\lambda \gg 1$, typically for cloud drops with visible radiation), Q^{ext} is about 2 (Fig. 2.9), yielding the extinction coefficient

$$b_\lambda^{ext} \simeq \frac{\pi d^2}{2} n. \quad (2.39)$$

Fig. 2.9 Evolution of the extinction efficiency as a function of the size parameter. Credit: Marilyne Tombette, CEREa

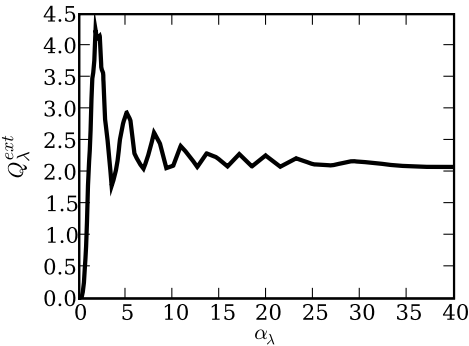


Table 2.4 Typical values of the surface albedo (visible radiation) for different surface types. Source: [67]

Surface	Albedo (visible)	Surface	Albedo (visible)
Liquid water	0.05–0.20	Grass	0.15–0.25
Fresh snow	0.75–0.95	Desert	0.20–0.40
“Old” snow	0.40–0.70	Forest	0.10–0.25
Sea ice	0.25–0.40	Bitume	0.05–0.20
Clouds	0.20–0.90	Urban	0.10–0.27

2.1.8 Albedo

For a given wavelength, the albedo of a surface (by extension of an atmospheric layer) is defined as the fraction of the incident radiation that is scattered backward. As shown in Table 2.4 for infrared radiation, the albedo varies according to the surface type.

We refer to Exercise 2.2 for the albedo of a two-layer atmosphere.

Exercise 2.2 (Albedo of a Two-Layer Atmosphere) We assume that the atmosphere is composed by a layer of albedo A_0 with respect to the solar radiation. Typically, the layer represents clouds. Consider a second layer of albedo A_1 (typically for the sulfate aerosols; Fig. 2.10), above the first layer. The second layer is supposed to be a perturbation of the first layer ($A_0 \gg A_1$). Calculate the global albedo. Hint: take into account multiple reflection between both layers.

Solution:

Let I be the incident solar radiation. We write R_n the reflected radiation (scattering backward to space), D_n the transmitted radiation from the upper layer to the lower layer, and U_n the reflected radiation from the lower layer to the upper layer, after n pairs of reflection on the layers.

After the first reflection, $R_0 = A_1 \times I$, $D_0 = (1 - A_1) \times I$, $U_0 = A_0 \times D_0$. The fluxes can be iteratively calculated with

$$U_n = A_0 \times D_n, \quad D_{n+1} = A_1 \times U_n = A_0 A_1 \times D_n, \quad R_{n+1} = (1 - A_1) \times U_n.$$

Thus, for $n \geq 0$,

$$R_{n+1} = A_0(1 - A_1)^2(A_0 A_1)^n \times I.$$

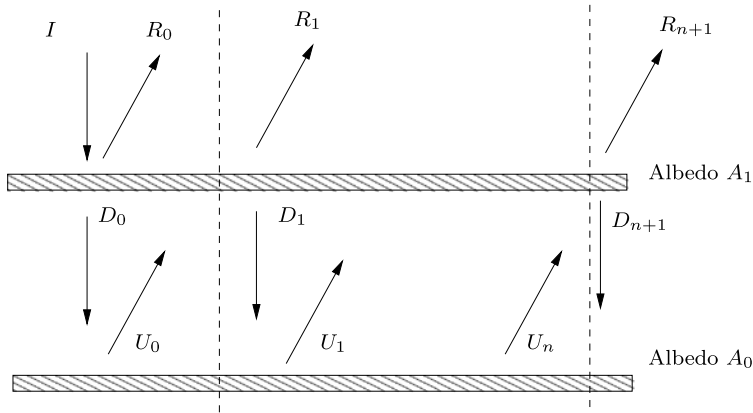


Fig. 2.10 Fate of the incident solar radiation (I) in a two-layer atmosphere

Summing over all the contributions due to reflection yields

$$R_0 + \sum_{n=0}^{\infty} R_{n+1} = \underbrace{\left(A_1 + \frac{A_0(1 - A_1)^2}{1 - A_0A_1} \right)}_A \times I.$$

Conserving the first-order terms in A_1 in an asymptotic expansion leads to

$$A \simeq A_1 + A_0(1 - 2A_1)(1 + A_0A_1) \simeq A_0 + A_1(1 - A_0)^2.$$

The global albedo is therefore not the sum of the layer albedos.

2.2 Applications to the Earth's Atmosphere

The concepts presented above are required for investigating the radiative properties of the atmosphere. The main application is the so-called *greenhouse effect*.

2.2.1 Solar and Terrestrial Radiation

2.2.1.1 Absorption Spectra

Calculating the absorption spectrum of the atmospheric compounds (namely of the absorption cross sections $\sigma_i^a(\lambda)$) is the objective of *spectroscopy*. This is based on the possible energy transitions for a given molecule. With the energy jumps ranked in an increasing order:

- the electronic transitions correspond to ultraviolet (UV) and visible radiation;

- the vibration transitions correspond to infrared (IR) radiation;
- the rotation transitions correspond to infrared and radio radiation.

For convenience, we do not cite the rotation-vibration transitions.

The vibration transitions can occur only for molecules presenting asymmetry. The geometrical structure of the molecules is therefore an important property for the interaction with the infrared radiation. This explains why CO₂, H₂O, N₂O or O₃ absorb and emit infrared radiation, on the contrary to O₂ or N₂. These gases are referred to as *greenhouse gases*.

The main absorption bands for the infrared radiation are shown in Table 2.5.

2.2.1.2 Absorption of Solar Radiation

Ionization The X-ray region of the electromagnetic spectrum (the most energetic radiation) is filtered in the ionosphere through the ionization process. Let A be a molecule or an atom. The ionization process reads

$$A + h\nu(\lambda) \longrightarrow A^+ + e^- . \quad (\text{R } 1)$$

Ionization requires high energies, defined by the concept of *ionization potential*. The ionization potential corresponds to the maximum of the wavelengths (thus to the minimum of the energies) for which ionization occurs. Table 2.6 shows the ionization potential for a few species and atoms.

Ionization takes place in the upper atmosphere. Once the X-ray region is filtered, the remaining part of the spectrum is not energetic enough so that ionization is no longer possible. As expected, the electron density is an increasing function of

Table 2.5 Main absorption bands for infrared radiation. To be compared to Fig. 2.12. Source: [141]

Species	band center (μm)	band (μm)
CO ₂	4.3	[4.1, 4.8]
	10.6	[8, 12]
	15	[12, 18]
O ₃	9.6	[9, 10]
H ₂ O	6.2	[5.3, 6.9]
stratosphere	7.4	[6.9, 8]
	8.5	[8, 9]
H ₂ O	15	[12.5, 20]
troposphere	24	[20, 29]
	57	[29, 100]
CH ₄	7.6	[6, 10]
N ₂ O	4.5	[4.4, 4.8]
	7.9	[7.4, 8.4]

altitude. For example, high values are responsible for the so-called *black out* that affects the communications of a space shuttle in the reentry phase (at an altitude of about 90–100 kilometers).

Ultraviolet and Visible Radiation The comparison between the spectrum of solar radiation at the top of the atmosphere and that at sea level is shown in Fig. 2.11.

For the ultraviolet solar radiation, the absorption is strong for molecular oxygen (O_2), ozone (O_3), water vapor (H_2O) and carbon dioxide (CO_2). These species, especially stratospheric ozone, filter the ultraviolet radiation, which anneals its adverse effects to health and vegetation. This motivates the focus on stratospheric ozone (Chap. 4).

Note the splitting between the ultraviolet and visible radiation:

- the shortwave solar radiations are absorbed in the ionosphere (X-ray region), in the mesosphere (Schumann-Runge continuum for O_2 , $\lambda \in [150, 200]$ nm) and in the stratosphere (Hartley continuum for O_3 , $\lambda \in [200, 300]$ nm);
- the atmosphere is transparent for the visible solar radiations: this property defines the so-called *atmospheric window*. This is a key point since it makes it possible to heat and to light the Earth’s surface.

2.2.1.3 Absorption of the Terrestrial Radiation

The longwave infrared radiations, corresponding to terrestrial and atmospheric emissions, are absorbed by water vapor (H_2O), CH_4 , CO_2 and O_3 . These gases are characterized by their strong absorption of the infrared radiations (*greenhouse gases*).

Table 2.6 Ionization potential (wavelength in nm)

O_2	H_2O	O_3	H	O	CO_2	N	N_2	Ar
102.7	99	97	91.1	91	90	85	79.6	79

Fig. 2.11 Radiance spectrum at the top of the atmosphere and at sea level, respectively. The difference between the two curves corresponds to the absorption of solar radiation in the atmosphere

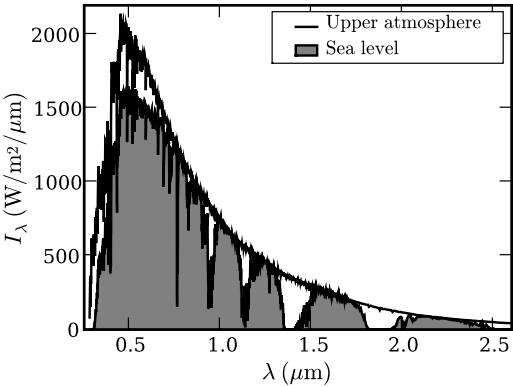


Figure 2.12 shows the radiance spectrum in the infrared region, as it would be measured by a sensor at the altitude of 70 kilometers, above a region with a temperature of 305 K. The spectrum is computed by a numerical model that solves the radiative transfer equation (MODTRAN) for a standard atmosphere (USA 1976, clear sky). The Planck's distributions for the blackbody emissions are plotted for a few temperatures.

Note the main absorption bands related to the greenhouse gases. A simplified model for the greenhouse effect is investigated in Sect. 2.2.3. The altitude at which the absorbing (and then emitting) gases are located can be obtained by comparing the spectrum with the Planck distribution. The corresponding emission temperature results in an altitude (by using the vertical distribution of temperature). We refer to Exercise 2.3 for the study of this peaked altitude, with the concept of absorption layer.

Remark 2.2.1 (Passive Remote Sensing) *Passive remote sensing* (by satellital platforms) is based on the absorption of the infrared radiations by the atmosphere. The spectrum that is measured by the satellite gives a direct indication of the vertical distributions of the atmospheric trace species (typically water vapor) and of the temperature. This information is useful for numerical weather prediction.

We refer to Sect. 6.4 for a general introduction to the underlying methods (data assimilation and inverse modeling). The *forward model* is provided by the radiative

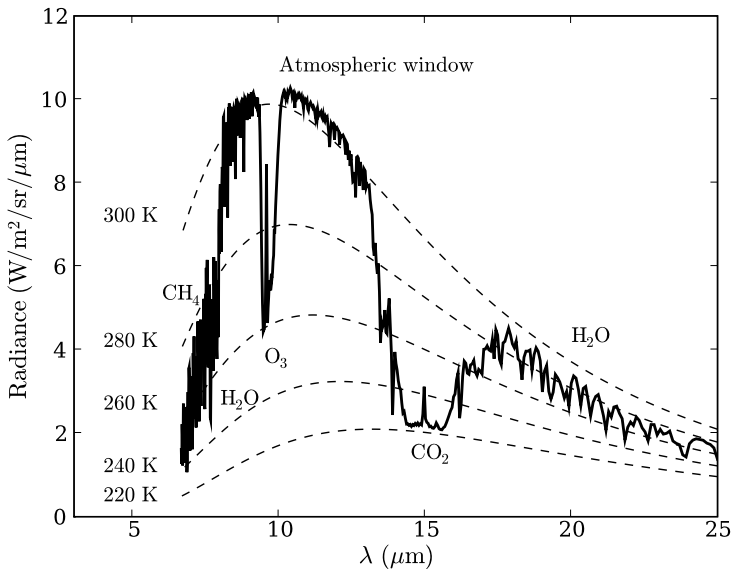


Fig. 2.12 Spectrum of the terrestrial infrared radiations, as measured by a sensor at the altitude of 70 km, above a surface with a temperature at 305 K. The spectrum is a virtual spectrum computed by the numerical model MODTRAN for the standard atmosphere (USA 1976, clear sky). The Planck's distributions (blackbody emissions) are given at 220, 240, 260, 280 and 300 K. The corresponding greenhouse gases are indicated near the absorption peaks

transfer equation, for example in the form (2.32), where the temperature distribution, $T(\tau)$, is supposed to be known. Inverse modeling results in an estimation of this distribution on the basis of radiance observations.

Exercise 2.3 (Chapman's Theory of Absorption Layers) This exercise aims at introducing the concept of *absorption layer*. Consider a molecule with a known absorption spectrum for solar radiation. The maximum of the absorption is supposed to be peaked for a given wavelength. Emission and scattering by the atmosphere are neglected and we only take into account absorption in the following.

The vertical profile of concentration is given by $n(z) = n_0 \exp(-z/H)$, with H a scale height and z the vertical coordinate (increasing with increasing altitudes). Let θ be the angle of the incident radiation with respect to the vertical direction, and s be the abscissa along the radiation direction (decreasing with increasing altitude), respectively.

1. Calculate the distribution of the absorption rate ($-dI/ds$).
2. Prove that there is a maximum at an altitude z_{max} . Comment.
3. Calculate z_{max} in the case of ozone (apply with $\theta = 0$).

Data for ozone:

$$-\sigma_a = 4 \times 10^{-17} \text{ cm}^2 \text{ molecule}^{-1};$$

$$-n(z) = n_0 \exp(-(z - z_0)/H) \text{ for } z \geq z_0 = 35 \text{ km}, n_0 = 10^{12} \text{ molecule cm}^{-3}, H = 5 \text{ km}.$$

Solution:

1. The evolution of the incident radiation is governed by the Beer-Lambert law, $dI/ds = -\sigma_a n(z(s))I$. At the top of the atmosphere, the boundary condition is $I(\infty)$. Since $dz = -\cos \theta ds$, this yields straightforward

$$I(z) = I(\infty) \exp\left(-\frac{H\sigma_a n_0}{\cos \theta} \exp(-z/H)\right).$$

The intensity (absorption, respectively) is an increasing (decreasing, respectively) function of the altitude, as expected. The absorption rate is given by

$$-\frac{dI}{ds} = \sigma_a n_0 I(\infty) \exp\left(-z/H - \frac{H\sigma_a n_0}{\cos \theta} \exp(-z/H)\right).$$

2. Setting to zero the second derivative of I gives the maximum of the absorption rate. The corresponding altitude is then

$$z_{max} = H \ln\left(\frac{H\sigma_a n_0}{\cos \theta}\right).$$

z_{max} depends on the incidence angle and on the properties of the absorbing medium (σ_a), but not on the incident radiation.

The absorption is a concave function of the altitude. Above z_{max} , the absorption is limited by the low value of the concentration; below z_{max} , the absorption is limited by the low value of the incident intensity since a large part of the intensity has been already absorbed.

3. For ozone, $z_{max} \simeq 50 \text{ km}$ (see Fig. 1.1, Chap. 1). This maximum of the absorption results in a maximum of an photolysis rate. We refer to Exercise 4.5 (Chap. 4) for an evaluation of the resulting increase in the atmospheric temperature.

2.2.2 Radiative Budget for the Earth/Atmosphere System

2.2.2.1 Solar Constant and Emission Effective Temperature

The solar constant of a given planet is defined by the solar radiation flux per unit area of the planet surface (Fig. 2.13, with the detail of the main notations). It can be calculated upon application of the Stefan-Boltzmann law to the Sun. The power emitted by the Sun (in W) is $4\pi R_s^2 \times \sigma T_s^4$ (with the Sun's radius $R_s = 6.96 \times 10^5$ km and the Sun's emission temperature $T_s = 5783$ K). At a distance r from the Sun, this generates a flux (expressed in W m^{-2})

$$S = \frac{R_s^2}{r^2} \sigma T_s^4. \quad (2.40)$$

With $r = 1.5 \times 10^8$ km (mean distance between the Sun and the Earth), we obtain the solar constant for the Earth, $S \simeq 1368 \text{ W m}^{-2}$.

For a given planet, the *emission effective temperature* is defined as the emission temperature of a blackbody in radiative balance with the radiative fluxes received by the planet. The radiative budget for the Earth/atmosphere system is calculated as shown in Fig. 2.13: the solar radiation is intercepted by a surface πR_t^2 (with R_t the Earth's radius), the fraction A is reflected back to space (with A the global albedo of the Earth/atmosphere system, $A \simeq 0.3$). Finally, upon division by the Earth's surface $4\pi R_t^2$, this gives the following radiative budget (in W m^{-2}),

$$\sigma T_e^4 = \frac{\pi R_t^2 S (1 - A)}{4\pi R_t^2} = \frac{S(1 - A)}{4}, \quad (2.41)$$

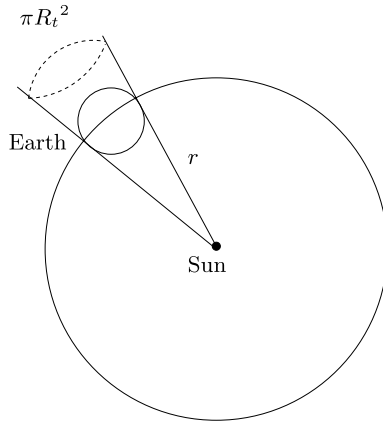


Fig. 2.13 Radiative flux received by the Earth (of radius R_t , at a distance r from the Sun). The solar flux per unit area of surface (expressed in W m^{-2}) received by a sphere of radius r and centered at the Sun, is $S = 4\pi R_s^2 \sigma T_s^4 / (4\pi r^2)$ with R_s and T_s the radius and the temperature of the Sun, respectively. The interception surface defined by the Earth is πR_t^2 , resulting in a received flux $\pi R_t^2 \times S$ and in a flux per unit area of the Earth's surface $\pi R_t^2 \times S / (4\pi R_t^2) = S/4$

with T_e the emission effective temperature of the Earth/atmosphere system. Rearranging yields

$$T_e^4 = \frac{S(1 - A)}{4\sigma}. \quad (2.42)$$

The emission effective temperature is therefore a function of the albedo and of the distance to the Sun (which defines the solar constant).

With $A \simeq 0.3$ we calculate $T_e \simeq 255$ K, to be compared with the mean temperature at the Earth's surface (about 288 K). The difference (33 K) corresponds to the greenhouse effect (which makes it possible to have a surface temperature greater than -18°C !) and results from an energy redistribution from the atmosphere to the ground.

The available flux at the Earth's surface is $S/4 \simeq 342 \text{ W m}^{-2}$. It is usually written as F_s .

Exercise 2.4 (Variation of the Solar Constant) Calculate the variation of the solar constant S during one year (the distance from the Sun to the Earth varies from 1.469 to 1.520×10^8 km)?

Solution:

We apply (2.40), which yields $S \in [1320, 1410] \text{ W m}^{-2}$. Thus, the variation is up to 90 W m^{-2} .

2.2.2.2 Energy Budget for the Earth/Atmosphere System

The temperature of the Earth/atmosphere system is mainly fixed by the radiative properties of the Earth and of the atmospheric compounds (gases, clouds and aerosols).

Let us express the global energy budget for the Earth/atmosphere system (Fig. 2.14). We consider the received solar energy, the energy fluxes for the Earth and the energy fluxes for the atmosphere.

The resulting budget is a global budget and does not take into account the seasons, the diurnal cycles (day/night) and the spatial location. Except for the solar flux, the relative uncertainties are at least of 10%. Thus, the fluxes are only crude estimations.

Received Solar Energy The solar energy is the only energy source for the Earth/atmosphere system. The incident solar radiation represents 342 W m^{-2} , to be split as follows.

- 77 W m^{-2} is reflected back to space by clouds and aerosols (namely 22%);
- 67 W m^{-2} is absorbed by gases and clouds (namely 20%);
- 168 W m^{-2} is scattered and then absorbed by the Earth (namely 49%);
- 30 W m^{-2} is reflected by the Earth and then scattered to space (namely 9%).

The planetary albedo is therefore about 0.31 (the reflected energy is 107 W m^{-2} , to be compared with the received energy, 342 W m^{-2}).

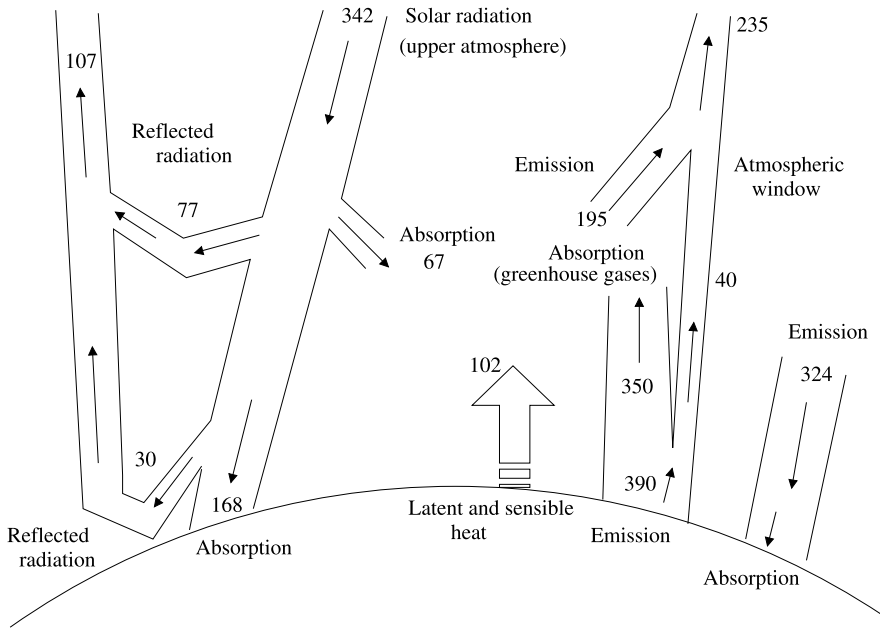


Fig. 2.14 Global energy budget for the Earth/atmosphere system. The fluxes are expressed in W m^{-2} . The values are indicative. Source: [74]

Earth's Energy Budget The energy fluxes for the Earth are related to:

- radiative energy;
- *sensible* heat (Chap. 3), connected to the vertical turbulent motions;
- *latent* heat, produced by the water cycle (see Exercise 3.1);
- heat conduction in the soil (neglected in a first approximation).

With the same units as above, the Earth absorbs 168 W m^{-2} in the shortwave solar radiation. It emits 390 W m^{-2} in the longwave radiation into the atmosphere.

As seen before, the emitted radiation is strongly absorbed by the atmosphere: actually, up to 350 W m^{-2} is absorbed (namely 90%) and 40 W m^{-2} (10%) is transmitted to space through the *atmospheric window*.

Moreover, the Earth receives 324 W m^{-2} from the longwave radiation emitted by the atmosphere. The whole part is supposed to be absorbed at the Earth's surface (in a first approximation).

The radiative budget is then positive for the Earth: *there is a gain of radiative energy for the Earth* ($168 + 324 - 390 = 102 \text{ W m}^{-2}$).

At equilibrium, the energy budget for the non-radiative part is therefore negative: the Earth has an energy loss (-102 W m^{-2}) by latent heat (water evaporation) and sensible heat (vertical turbulent motion).

Atmosphere's Energy Budget The atmosphere absorbs 67 W m^{-2} in the short-wave solar radiations and 350 W m^{-2} in the longwave terrestrial radiations. It emits 519 W m^{-2} in the longwave radiations (including 324 to the Earth and 195 to space).

The radiative budget for the atmosphere is therefore negative ($350 + 67 - 519 = -102 \text{ W m}^{-2}$): *the atmosphere has a loss of radiative energy*. At equilibrium, the energy gain is provided by latent and sensible heat fluxes (102 W m^{-2} , coming from the Earth).

The Earth/atmosphere system absorbs 235 W m^{-2} from the solar radiation ($168 + 67$), to be compared with the value given in Table 2.1.

2.2.3 Greenhouse Effect

2.2.3.1 A Toy Model for the Greenhouse Effect

The concept of greenhouse effect was introduced in order to justify the elevated temperature at Venus' surface (more than 700 K, see Exercise 2.5), as compared to the emission effective temperature (230 K): the hypothesis was formulated by Rupert Wildt in the 1930s and Carl Sagan in 1962, before the confirmation by the measurements of the CO_2 mixing ratio in the atmosphere of Venus.

Exercise 2.5 (Jupiter, Mars and Venus) The characteristics of Jupiter, Mars and Venus are given in Table 2.7. Assess the possibility of a greenhouse effect for these planets. What could be the other source of energy for Jupiter?

Solution:

We use (2.40) to get the general formula

$$T_e = T_s \sqrt{\frac{R_s}{2r}} (1 - A)^{0.25}, \quad (2.43)$$

with A the planet albedo and r the distance from the Sun. This gives $T_e = 88, 232$ and 216 K for Jupiter, Venus and Mars, respectively. Thus, there exists a strong greenhouse effect for Venus on the contrary to Mars. The composition of the Jovian atmosphere does not support the existence of a greenhouse effect. The high value of the surface temperature can be explained by internal energy sources. If ΔE_{int} stands for the internal energy source, the energy balance should read

$$\sigma T^4 = \sigma T_e^4 + \Delta E_{int},$$

Table 2.7 Characteristics of Jupiter, Venus and Mars

Planet	Distance (km) from the Sun	Albedo	C_{CO_2} (%)	T at ground (K)
Jupiter	7.8×10^8	0.73		130
Venus	1.08×10^8	0.75	0.96	700
Mars	2.28×10^8	0.15	0.95	220

namely $\Delta E_{int}/(\sigma T_e^4) = (T/T_e)^4 - 1 \simeq 4$. The internal energy source is up to four times as large as the solar energy flux. For the Earth, the contribution due to the internal energy (geothermy) can be neglected (Table 2.1).

Consider the atmosphere as a virtual layer at a given distance from the Earth's surface. Let us assume that nothing happens in the region between the surface and the layer (Fig. 2.15).

From the radiative properties of the atmosphere (strong absorption of the infrared radiations and atmospheric window for the visible radiations), we assume that:

- the layer and the Earth are at radiative equilibrium: in a first approximation, we neglect the non-radiative energy flux;
- the layer reflects a fraction A of the incident solar radiation F_s . It absorbs a fraction a_S and transmits to the Earth a fraction $(1 - a_S)$ of the remaining radiation $(1 - A)F_s$. The Earth is supposed to absorb the whole received radiation;
- the Earth emits longwave radiations U (*up*): a fraction (a_T) is absorbed by the layer while the remaining part $(1 - a_T)$ is transmitted to space;
- the layer is then heated and emits a radiation D (*down*): a fraction a is transmitted to the Earth and then absorbed.

Let us investigate the sensitivity of the Earth's temperature (T) with respect to the absorption coefficient of the layer for the terrestrial radiation (a_T).

Taking into account the previous data (Fig. 2.14) yields

$$a_T = \frac{350}{390}, \quad a_S = \frac{198}{265}, \quad a = \frac{324}{519}. \quad (2.44)$$

The budget energy for the Earth and the atmospheric layer reads

$$\begin{cases} (1 - a_S)(1 - A)F_s + aD = U = \sigma T^4 \\ a_S(1 - A)F_s + a_T U = D. \end{cases} \quad (2.45)$$

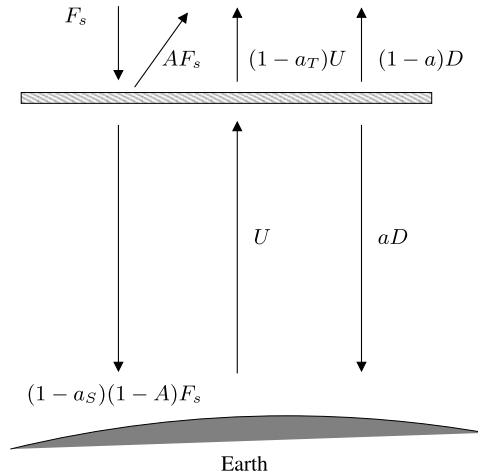


Fig. 2.15 A toy model for the greenhouse effect

Thus,

$$\sigma T^4 = U = \frac{(1 - a_S) + a a_S}{1 - a a_T} (1 - A) F_s. \quad (2.46)$$

The function $T(a_T)$ is an *increasing* function with respect to the absorption coefficient of the layer (a_T). The more absorbing the layer is, the higher the Earth's temperature is: this is the *greenhouse effect*, to be measured by the difference between the emission effective temperature T_e given by (2.42) and the surface temperature T . This gives straightforward

$$T = \left(\frac{(1 - a_S) + a a_S}{1 - a a_T} \right)^{0.25} T_e. \quad (2.47)$$

As $T_e \simeq 255$ K, we get $T \simeq 288$ K (not far from the observed value).

2.2.3.2 Radiative Forcing, Feedbacks and Global Warming Potentials

The estimation of the impact on the temperature, and more generally on the climate, is an active research topic. It can also generate controversies since the scientific results play a leading role for the decision-making. We refer to the IPCC reports (*Intergovernmental Panel on Climate Change*, [106]). A key point is the attention paid to the “robustness” of the results. What are the levels of uncertainties? What is the level of scientific understanding (LOSU)?

In the following, we focus on a few key elements, namely the concepts of *radiative forcing*, *feedbacks* and *global warming potential*.

Radiative Forcing The *radiative forcing* is defined in the following way ([106]):

The radiative forcing of the surface-troposphere system due to perturbation in or the introduction of an agent (say, a change in greenhouse gas concentrations) is the change in net (down minus up) irradiance (solar plus long-wave; in W m^{-2}) at the tropopause AFTER allowing the stratospheric temperatures to readjust to radiative equilibrium, but with surface and tropospheric temperatures and state held fixed at the unperturbed values.

For example, a modification of the albedo perturbs the balance (2.41). In coherence with the definition above (*down minus up*), the balance reads

$$F = F_s(1 - A) - \sigma T_e^4 = 0. \quad (2.48)$$

Applying a perturbation ΔA for the albedo leads to a forcing $\Delta F = -F_s \Delta A$. An increase in the albedo results, as expected, in a negative radiative forcing (cooling effect).

Similarly, a modification ΔF_s of the received solar flux $F_s = S/4$ leads to a forcing $\Delta F = \Delta F_s(1 - A)$. An increase in F_s results in a positive radiative forcing.

The impact on the effective temperature T_e (and then on the surface temperature T) can be estimated (see Exercise 2.7 for a more rigorous approach) by assuming

that the radiative forcing is an energy flux to be added to the received solar energy. The resulting equilibrium is

$$F_s(1 - A) + \Delta F - \sigma(T_e + \Delta T_e)^4 = 0. \quad (2.49)$$

The *climate sensitivity parameter* is often written as λ_0 ⁴ and is defined by

$$\lambda_0 = \frac{\Delta T_e}{\Delta F}. \quad (2.50)$$

It is expressed in $\text{K}(\text{W m}^{-2})^{-1}$. Actually, the resulting value, about 0.3 (see Exercise 2.6), is an underestimation because couplings and *feedbacks* are not taken into account. We refer to Exercise 2.7 for the concept of feedbacks.

Exercise 2.6 (Estimation of the Climate Sensitivity Parameter) Calculate the sensitivity of the emission effective temperature with respect to a radiative forcing.

Solution:

Linearizing (2.49) yields $\Delta F \simeq 4\sigma T_e^3 \Delta T_e$, namely

$$\lambda_0 = \frac{\Delta T_e}{\Delta F} \simeq \frac{1}{4\sigma T_e^3}.$$

As $T_e = 255 \text{ K}$, we obtain $\lambda_0 \simeq 0.27 \text{ K}(\text{W m}^{-2})^{-1}$. This value does not take into account the feedbacks and is an underestimation.

This concept can be generalized to the radiative forcing related to a greenhouse gas, let us say X_i . Increasing the concentration of X_i results in decreasing the outgoing flux of the terrestrial radiations (we omit the possible feedbacks). Equivalently, this can be viewed as an increase in the incoming solar radiation. This calculation has to be carried out with the other parameters considered at constant values. A few values, taken from the IPCC report of 2001 ([106]), are shown in Table 2.8. Note the large uncertainties related to aerosols (see Sect. 2.2.4). For example, the sign of the radiative forcing related to mineral aerosols (e.g. dust) is not fixed (Problem 2.1).

Feedbacks The sensitivity, as presented above, does not take into account the resulting modifications of the other components of the Earth/atmosphere system, due to radiative forcing and temperature modification. The key feedbacks to describe are listed below.

- **Water Vapor Feedback**

A warmer atmosphere is wetter, which results in an increasing greenhouse effect related to water vapor (positive feedback). Actually, the saturation vapor pressure of water vapor is an increasing function of temperature, which favors the gas-phase state of water (Sect. 5.2.2).

Moreover, the increasing temperature can amplify the water evaporation from the oceans. An extreme case corresponds to the so-called *runaway greenhouse effect*.

⁴This is a standard notation (not to be mixed up with that used for wavelength).

The evaporation of water from oceans is then no longer compensated by cloud formations and subsequent precipitations, since the saturation vapor pressure is too high (due to the high values for the temperature). Water evaporates but cannot condense in the atmosphere (Fig. 2.16). This runaway is the hypothesis that is usually formulated for justifying the lack of water at Venus' current surface. Actually, the effective temperature of Venus was, initially, higher than that of the Earth.

- Albedo

The resulting modification of the albedo, due to the modification of the Earth's surface (e.g. the decrease of the ice cover), is another positive feedback. A warmer atmosphere results in ice melting, which contributes to decrease the albedo and therefore to increase the absorption of solar radiation at the Earth's surface.

- Clouds and Aerosols

Taking into account the impact of the cloud cover is more complicated. The clouds reflect the solar radiation but, meanwhile, they also absorb part of the infrared radiations. The impact of aerosols is a major uncertainty (Sect. 2.2.4).

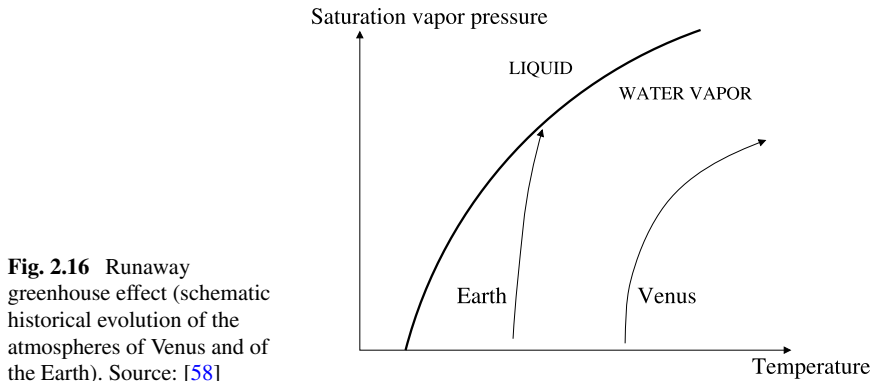
The concept of feedback is formalized in Exercise 2.7.

Exercise 2.7 (Formalization of the Feedback Concept) A simple way for formalizing the concept of feedback is to consider that the temperature (T) is a function not only of the radiative flux F but also of the other variables, $\{x_i\}_i$ (e.g. albedo, cloud cover, concentrations of greenhouse gases, ...): $T = f(F, \{x_i\}_i)$. Assuming that the variables x_i also depend on T , calculate the sensitivity dT/dF .

Solution:

The sensitivity reads

$$\lambda = \frac{dT}{dF} = \underbrace{\frac{\partial T}{\partial F}}_{\lambda_0} + \sum_i \frac{\partial T}{\partial x_i} \frac{\partial x_i}{\partial F}.$$



Taking into account the dependence upon T , $x_i(T)$, we obtain $\partial x_i/\partial F = dx_i/dT \times dT/dF$. Thus,

$$\lambda = \frac{\lambda_0}{1 - \sum_i f_i}, \quad f_i = \frac{\partial T}{\partial x_i} \frac{dx_i}{dT}.$$

The variable f_i is the so-called *feedback factor* for the variable x_i (connected to a physical process). It is dimensionless. For the calculation of f_i , we have to distinguish $\partial T/\partial x_i$, corresponding to the temperature dependence on the variable (through the radiative balance), from dx_i/dT , corresponding to the fact that the variable is driven by the temperature (through the physical and chemical atmospheric processes). If both values are positive, (that is to say if an increase in the temperature results in an amplification of the process, leading to an increase in the temperature), we have a positive feedback.

From the IPCC works ([106], Table 2.8), the antropogenic radiative forcing between 1750 (preindustrial times) to 1998 can be estimated as 2.43 W m^{-2} (including 1.46 W m^{-2} for CO_2 , 0.48 W m^{-2} for CH_4 , 0.34 W m^{-2} for halogen compounds and 0.15 W m^{-2} for N_2O). For an increase in the temperature estimated as 0.6 K , the climate sensitivity parameter is therefore about 0.25 .

Table 2.8 Mean yearly radiative forcing between 1750 and 2000, as estimated by the IPCC works in 2001. “LOSU” stands for *level of scientific understanding*. Source: [106]

Species X_i	ΔF_{X_i} (W m^{-2})	Uncertainties	LOSU
Greenhouse gases	2.43	10%	High
incl. CO_2	1.46	–	–
incl. CH_4	0.48	–	–
incl. N_2O	0.14	–	–
incl. halogens	0.34	–	–
Stratospheric O_3	–0.15	67%	Medium
Tropospheric O_3	0.35	43%	Medium
Sulfate aerosols (direct)	–0.4	[–0.8, –0.2]	Low
Biomass burning aerosols (direct)	–0.2	[–0.6, –0.07]	Very low
Soot (elemental carbon, direct)	0.1	[0.03, 0.3]	Very Low
Organic aerosols (direct)	–0.1	[–0.3, –0.03]	Very Low
Mineral aerosols	[–0.6, 0.4]	–	Very Low
Indirect effect of aerosols	[–2, 0]	–	Very Low
Condensation trails (aircrafts)	0.02	350%	Very Low
Cirrus formation (aircrafts)	[0, 0.04]	–	Very Low
Surface albedo (land use cover)	–0.2	100%	Very Low
Solar activity	0.3	67%	Very Low

Global Warming Potential A third key concept is the atmospheric residence time of the species. For a species X_i , the *global warming potential*, GWP_i , is defined by comparing, over a time interval $[0, t_f]$, the radiative forcing resulting from a 1 kg emission of X_i at $t = 0$, with that resulting from the same emission of a reference species (usually carbon monoxide CO_2). Thus,

$$GWP_i = \frac{\int_0^{t_f} \Delta F_{X_i}(t) \, dt}{\int_0^{t_f} \Delta F_{\text{CO}_2}(t) \, dt}.$$

(2.51)

We refer to Table 2.9 for a few values (note that GWP depends on t_f). For example, if the final time is 100 years, reducing the emissions of CFC-11 by 1 kg is as efficient as a 4600 kg emission reduction for CO_2 .

Actually, this indicator only takes into account the so-called *direct* effects. It is sometimes referred to as *direct GWP*. It does not describe the indirect effects, resulting from the physical and chemical processes induced by the emission of a given species for other species. The *indirect* GWP is difficult to estimate. For example, the emission of methane (CH_4) has several indirect effects, among which:

- an increased chemical production of ozone (this indirect effect is estimated to be up to 25% of the direct effect);
- an increased production of water vapor in the stratosphere (5% of the direct effect).

2.2.4 Aerosols, Clouds and Greenhouse Effect

The uncertainties related to the radiative behavior of the aerosols and clouds are a challenging issue for providing an accurate estimation of the anthropogenic greenhouse effect.

Table 2.9 *Direct* global warming potential (normalized with respect to CO_2) for a few species, at 20, 100 and 500 years. Source: [106]

Species	Residence time (year)	GWP	GWP	GWP
		at 20 years	at 100 years	at 500 years
CO_2	100	1	1	1
CH_4	12	62	23	7
N_2O	114	275	296	156
CFC-11	45	6300	4600	1600
CFC-12	100	10200	10600	5200
CFC-13	640	10000	14000	16300

2.2.4.1 Direct Effect of Clouds

The clouds play a leading role in the radiative forcing with two opposite effects:

- a cooling effect with respect to the solar radiation.
They constitute a scattering medium for the solar radiation and contribute to the global albedo. The reflection of the incoming solar radiations back to space depends on the cloud type and on the microphysical properties: the cloud albedo (for solar radiation) varies from 0.20 (for thin stratus) to 0.90 (for cumulus), as shown in Table 2.4. It is usually estimated that the cloud contribution is up to 0.15 for the albedo of the Earth/atmosphere system, namely the half of the total albedo.
For the “current” atmosphere, the resulting cloud contribution to the radiative budget is estimated to be -50 W m^{-2} (for the solar radiation).
- a greenhouse effect for the infrared radiation.
On the contrary, the clouds increase the scattering of the shortwave radiations to the Earth’s surface. The key point is that they also increase the emissivity and the absorptivity of the atmosphere for longwave radiations ($\epsilon \simeq 0.97$ for clouds). Hence, the clouds act as strong “greenhouse gases”. Note that they emit at temperatures lower than the temperature surface (or than the temperature for a clear sky). The resulting contribution to the radiative balance is estimated to be about $+25 \text{ W m}^{-2}$.

The aggregated effect is then a cooling effect (with a contribution of about -25 W m^{-2} for the radiative budget). A more accurate estimation of this impact is required: remember that a doubling of the CO_2 mixing ratio results in a perturbation of a few W m^{-2} .

The impact on the clouds resulting from a modification in the atmospheric composition is difficult to estimate, which provides another illustration of the concept of feedback.

For the solar radiation, the increase of the water vapor mixing ratio results in an increase of the cloud cover, and then of the global albedo (cooling effect). Meanwhile, it can also result in an increase of precipitations, leading to a decreasing cloud lifetime and therefore to a decreasing albedo.

For the infrared radiation, the clouds take part in the greenhouse effect. For a finer estimation, the cloud altitude has to be taken into account: for example, clouds at high altitudes (e.g. cirrus) have a warming effect.

2.2.4.2 Direct Effects of Aerosols

Cooling Effect of Sulfate Aerosols Due to their radiative properties, the sulfate aerosols have a direct effect for the solar radiation. This is a cooling effect due to an increase in the planetary albedo. This is sometimes referred to as the *whitehouse effect* ([127]).

Decreasing temperatures have been measured after eruption of the Pinatubo Mount (1991). The eruption resulted in an increase in the stratospheric sulfate concentrations: the resulting radiative forcing was estimated to be up to -4 W m^{-2} in 1992 with a fast decrease down to -0.1 W m^{-2} in 1995. The cooling effect for the temperature was estimated to be of a few tenths of K.

The radiative forcing related to the increase in the albedo (to be applied for the effects above) is $\Delta F = -F_s \Delta A$. With Exercise 2.8, a coarse estimation for the aerosol albedo is about 2×10^{-2} . Considering that 25% of the aerosols are anthropogenic aerosols, we obtain an albedo connected to the anthropogenic aerosols of $A_1 = 5 \times 10^{-3}$. The perturbation for the global albedo cannot be calculated directly. The calculation of the albedo for a two-layer atmosphere is detailed in Exercise 2.2. The resulting perturbation for the global albedo is actually $\Delta A = A_1(1 - A_0)^2$, where A_0 is the albedo of the other atmospheric compounds (0.3 in a first approximation).

Exercise 2.8 (Estimation of the Aerosol Albedo) Estimate, for the aerosols, the contribution to global albedo with respect to the solar radiation.

Data:

- total optical depth associated to the aerosols: $\tau \simeq 0.12$ (mean value above the oceans, [57]);
- suppose that a fraction $\beta = 23\%$ of the scattered radiation is scattered back to space).

Solution:

The incident radiation, I , can be split in a transmitted radiation, $\exp(-\tau)I$, and in a scattered radiation, $(1 - \exp(-\tau))I$. A fraction β of the scattered radiation is reflected back to space, resulting in an albedo $A_1 = \beta(1 - \exp(-\tau)) \simeq \beta\tau$. Thus, $A_1 \simeq 0.026$.

Finally, we obtain $\Delta F \simeq -0.85 \text{ W m}^{-2}$. Note that this value is similar to the sum of the direct radiative forcings related to anthropogenic aerosols in Table 2.8.

Hence, the particulate pollution (a more localized pollution) has reduced part of the anthropogenic greenhouse effect. The indirect effect of an improvement of the local air quality is an increase of the anthropogenic greenhouse effect: this is an example of an *atmospheric dilemma* (see Introduction and Exercise 2.9). Another application of the cooling effect related to aerosols is the so-called *nuclear winter* (the strong cooling induced by a nuclear war; Problem 2.4).

Exercise 2.9 (Climate Engineering and Greenhouse Effect) In order to counterbalance the reduction of the cooling effect related to sulfate aerosols, due to the improvement of the local air quality, P. J. Crutzen (who was awarded the Nobel Prize in 1995), suggests that we emit sulfate particles into the stratosphere, “[as an] *escape route against strongly increased temperature*” (see Introduction). The stratospheric emission is motivated by the higher residence times of the stratospheric particles (from 1 to 2 years, versus one week in the troposphere, Chap. 5). This exercise aims at giving the basis of Crutzen’s arguments.

In 1991, the volcanic eruption of the Pinatubo Mount emitted about 10 Tg of sulfur into the stratosphere. A few months later, 6 Tg were still in the stratosphere.

This resulted to a radiative forcing of about -4.5 W m^{-2} and to a diminution of the mean surface temperature of about 0.5 K in 1992.

Assume that the cost for sending 1 Tg S into the stratosphere is about 25 billions of dollars (on the basis of technologies supposed to be available). Calculate the project cost in order to compensate the radiative forcing due to the improvement of air quality (supposed to be about $+1.5 \text{ W m}^{-2}$) and that due to a doubling of CO_2 concentration (supposed to be about $+4 \text{ W m}^{-2}$). For indication, the magnitude of the current anthropogenic sulfur emissions is 55 Tg year^{-1} .

Note that there are possible adverse effects of such emissions. For example, this could result in an increase of the stratospheric ozone destruction (as observed after the Pinatubo eruption), due to the role of the aerosol sulfates in heterogeneous processes (Sect. 4.2).

Solution:

Using the data for the Pinatubo eruption, with a linear assumption, the radiative forcing induced by a 1 Tg S emission is about -0.75 W m^{-2} (4.5/6). As the lifetime varies from 1 to 2 years in the stratosphere, it is then required to inject from 1 to 2 Tg S per year into the stratosphere, so that the effect due to the improvement of the local air quality could be compensated. The resulting cost ranges from 25 to 50 billions of dollars. For compensating the doubling of CO_2 concentration, one should emit from 2.5 to 5 Tg S per year, with an annual cost ranging from 60 to 120 billions of dollars.

To know more ([26]):

P. CRUTZEN, *Albedo enhancement by stratospheric sulfur injections: a contribution to resolve a policy dilemma?* Climatic Change, **77** (2006), pp. 211–219

Sensitivity with Respect to the Aerosol Composition: Black Carbon and Liquid Water Content Actually, the radiative properties of aerosols depend on the size, on the chemical composition, on the mixing state (the way the components are mixed) and on the liquid water content. We refer to Problem 2.1 for the study of the sensitivity of the direct effect with respect to the aerosol chemical composition.

We investigate two characteristics in order to illustrate the related uncertainties: the first one is related to black carbon, the second one to the aerosol liquid water content.

Even if its mass contribution is rather low, *black carbon* has a major radiative impact that is difficult to assess. The resulting radiative forcing is positive since black carbon absorbs the infrared radiations. The amplitude is however highly uncertain: the aerosol mixing state strongly impacts the radiative forcing, with a multiplying factor up to 2 or 3 (Table 2.10). In case of *internal mixing*, the aerosol species are well mixed and are represented by one or a few families. In case of *external mixing*, the aerosols species are supposed not to be mixed (Sect. 5.1.1.4). Another key property is the aerosol geometry: in the so-called carbon core/shell model, the aerosol core is composed of black carbon while the surface shell is composed of organic and inorganic species (Fig. 2.17).

As shown in Table 2.10, the radiative forcing due to black carbon increases from the case of external mixing to the case of internal mixing. This results straightfor-

Fig. 2.17 Schematic representation of the aerosol mixing state: external mixing, carbon core/shell model, internal mixing. The black part stands for carbon (soot, elemental carbon or *black carbon*)

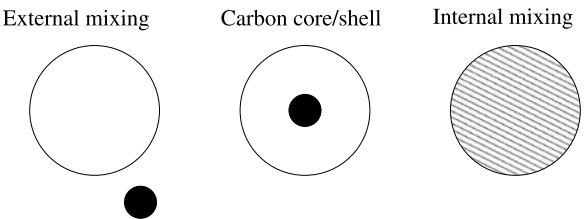


Table 2.10 Radiative forcing (in W m^{-2}) due to carbon aerosols (soot), as a function of the mixing state. Sources: [62, 63]

Mixing state	[62]	[63]
external mixing	0.27	0.31
carbon core/shell	0.54	0.55
internal mixing	0.78	0.62

ward from the ranking of the extinction coefficients. To date, many studies have been based on the assumption of external mixing (easier to implement for modelers). It may be therefore possible that the positive radiative forcing related to black carbon has been underestimated. The values obtained with the carbon core/shell model in the case of multiple internally-mixed families (due to hetero-coagulation of aerosols; probably the most realistic assumption), could rank black carbon as the second contributor to the greenhouse effect (Table 2.8). This could therefore motivate the reduction of black carbon emissions.

Assessing the impact of the aerosol liquid water content is another challenging issue. For aerosols containing hydrophilic compounds (that is, compounds that favor water conditions for appropriate values of the relative humidity), an increase in the humidity results in an increase in the aerosol size, which affects the radiative properties. A typical illustration is given in Fig. 2.18. An accurate estimation of this effect requires an accurate description of humidity and of the aerosol microphysical properties. One key property is the so-called deliquescence relative humidity, defined as the relative humidity above which water condensation takes place (Sect. 5.1, Chap. 5).

2.2.4.3 Indirect Effects of Aerosols

Part of the aerosol distribution provides the so-called *cloud condensation nuclei*, from which the cloud drops are produced (Sect. 5.2.3). Since the clouds affect the radiation, especially the solar radiations, this generates an *indirect effect* related to aerosols (Table 2.12). A key point is the decisive role of the cloud microphysical properties that are connected to aerosols: for example, the cloud albedo with respect to the visible radiations is a decreasing function of the drop size, or, equivalently, an increasing function of the drop number density (Twomey effect, Problem 2.2 and Fig. 2.19). These effects have been observed during the international field campaign INDOEX, devoted to the study of the Asian “brown cloud” (Exercise 2.10 and Table 2.11).

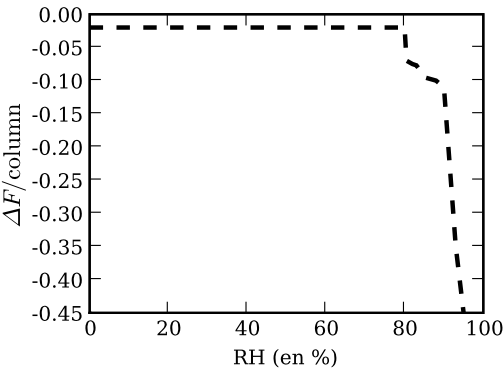


Fig. 2.18 Sensitivity of the radiative forcing (normalized with respect to the aerosol column; expressed in $\text{W m}^{-2}/(\text{mg m}^{-2})$) with respect to the relative humidity. The size distribution is centered at a dry radius $0.1\text{ }\mu\text{m}$; the aerosol is composed of 90% sulfate and 10% black carbon (carbon core). The water condensation occurs for a relative humidity above 80% (deliquescence relative humidity for ammonium sulfate, Table 5.6). Source: [85]

Table 2.11 Microphysical characteristics measured over the Indian Ocean: comparison between a *pristine* cloud and a *brown* cloud (Exercise 2.10) with the same liquid water content $L = 0.15\text{ g m}^{-3}$. The aerosols are taken into account for a diameter $d_p \geq 50\text{ nm}$. Source: [118]

Cloud	aerosol number density	cloud drop number density	effective radius (r_e)
pristine cloud	500 cm^{-3}	90 cm^{-3}	$r_e \geq 7.5\text{ }\mu\text{m}$
brown cloud	1500 cm^{-3}	315 cm^{-3}	$r_e \leq 6.5\text{ }\mu\text{m}$

Table 2.12 Indirect effects of aerosols. ΔF_0 stands for the radiative forcing at the Earth’s surface and p_0 is the rain intensity (expressed in mm hr^{-1}). Source: [90]

Effect	description	impact
Indirect effect of aerosols for clouds with a fixed liquid water content (cloud albedo, Twomey effect)	Increasing reflection of the solar radiation for small drops	$\Delta F_0 < 0$
Indirect effect of aerosols for clouds with a variable liquid water content (lifetime effect)	Decreasing precipitations and increasing cloud lifetime for small drops	$\Delta F_0 < 0, p_0 \downarrow$
Semi-direct effect	The absorption of solar radiation (soot) can increase the cloud drop evaporation	$\Delta F_0 < 0?, p_0 \downarrow$

Exercise 2.10 (Brown Clouds) Several studies, especially over the southern Asia and the Indian Ocean, have indicated the existence of extended persistent plumes of particulate matter, downwind urban polluted areas. These plumes are usually re-

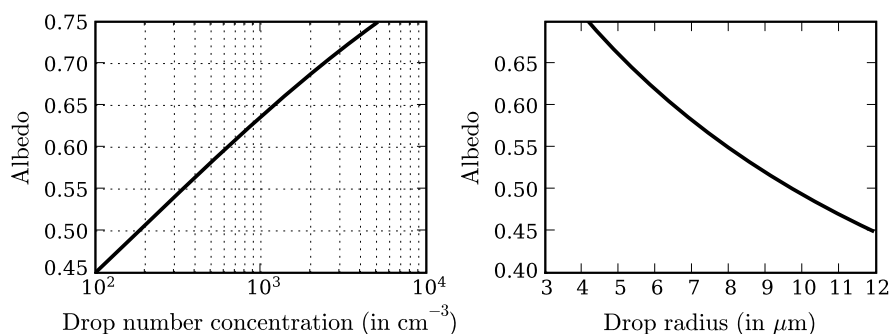


Fig. 2.19 Evolution of the cloud albedo as a function of the cloud drop number density and of the cloud drop effective radius. The cloud drop distribution is supposed to be monodispersed. See Problem 2.2

ferred to as *atmospheric brown clouds* (ABC). For example, the Asian brown cloud has a thickness up to 3 kilometers. Similar clouds can be measured over the North Atlantic Ocean (North Atlantic plume), over north-eastern Europe, over the Pacific Ocean (Chinese plume) and over the South Atlantic Ocean (biomass burning plume from the Amazonian forest).

There are many impacts. First, the resulting radiative forcing is negative ($-20 \pm 4 \text{ W m}^{-2}$ for the Asian brown cloud). Second, the water cycle is modified: the cloud drops are smaller and their evaporation may be also increased (according to a few measurements). Table 2.11 gives a few data for a pristine cloud and a brown cloud. The observational data indicate that the brown cloud is much stronger during the dry season and in the tropical zone. Why?

Solution:

Precipitation is weaker during the dry season, which results in a decrease of rain scavenging (Chap. 5). Moreover, there are always residual precipitations at mid-latitudes.

To know more ([118, 119]):

V. RAMANATHAN AND P. CRUTZEN, *Atmospheric Brown Clouds*, Atmos. Env., (2003), pp. 4033–4035

V. RAMANATHAN ET AL., *Indian Ocean Experiment (INDOEX): an integrated analysis of the climate forcing and effects of the great Indo-Asian haze*, J. Geophys. Res., **106** (2001), pp. 28371–28398

Contradictory effects resulting from the same cause may also occur. For example, an increase in the aerosol number results in an increase in the cloud drop number. This induces a reduction of the precipitation efficiency and, meanwhile, an increase in the cloud lifetime. A first impact is the decrease of snow falls (due to the reduced precipitation efficiency; microphysical effect). The second impact is the increase in reflection of the solar radiation, leading to a decrease in the temperature, and then in increasing snow falls (radiative effect). The global impact, as far as the snow falls are concerned, is then ambiguous ([90]).

2.2.4.4 Scientific Controversies

Other effects have been subject to scientific controversies during the last years. The typical example is the case of the *cosmic rays*. H. Svensmark ([140]) formulated the hypothesis that there was a correlation between the cosmic rays (depending on the solar activity) and the formation of cloud condensation nuclei, through ionization processes, especially for low clouds (those involved in the reflection of the solar radiation, namely implied in a cooling effect). Since the observational data are likely to show a decrease of 25% for the cosmic rays during the last century, this could explain the climate change. These works have generated scientific controversies. First, there is no well-defined microphysical processes that could support this hypothesis. Second, a few studies, using new data (after 1995) have shown that the correlation between the cosmic rays and the cloud cover may not be significant ([79]).

There are other scientific debates. For instance, a few studies investigate the possible underestimation of the solar radiation absorption by clouds (down to 40% of the usual value; [40] and [88], among many other references). New observational data (sometimes used by the same scientific teams) seem to indicate that this issue is not prevailing.

2.2.5 Atmospheric Pollution and Visibility

The reduction in visibility is one of the most spectacular impacts resulting from a pollution event in urban areas. This is usually defined with the concept of *visual contrast*. Consider a dark body in a clear medium. The visual contrast, C_v , is the relative difference between the intensity (radiance) of the body and that of the medium. It depends on the distance (x) between the observer and the body (located at $x = 0$). Let I_b be the intensity related to the medium, supposed to have a constant value, and I be that of the object, respectively. Thus, the visual contrast is

$$C_v(x) = \frac{I_b - I(x)}{I_b}. \quad (2.52)$$

Since the body is supposed to absorb all radiations (it does not emit nor reflect radiation), $I(0) = 0$ and the maximum of the visual contrast is met at the body location: $C_v(0) = 1$. For $x > 0$, there are two medium contributions to the evolution of I : first, there is a scattering of the ambient intensity due to gases and particles, and, second, there is an extinction of I (due to absorption and scattering). The first contribution is evaluated by $b^{ext} I_b$ while the second one is in the form $-b^{ext} I$ with b^{ext} the extinction coefficient (supposed to be the scattering coefficient), namely

$$\frac{dI}{dx} = b^{ext} I_b - b^{ext} I. \quad (2.53)$$

As I_b is constant (it does not depend on x), we obtain an equation similar to the Beer-Lambert law,

$$\frac{dC_v}{dx} = -b^{ext} C_v, \quad (2.54)$$

whose solution is $C_v(x) = \exp(-b^{ext}x)$.

The decrease in visibility is usually estimated by a distance, written as x_v , corresponding to the distance at which the reduction in the visual contrast is below a given threshold. The threshold is defined so that a “mean” observer would not see the contrast between the body and the medium. The threshold is typically 2%. As $\ln(50) = 3.912$, this yields the so-called Koschmieder equation (1922),

$$x_v = \frac{3.912}{b^{ext}}. \quad (2.55)$$

The contributions for the extinction include Rayleigh scattering (due to gases except NO_2), extinction due to NO_2 and that due to aerosols. Nitrogen dioxide colors the polluted plumes in red, brown or yellow (Fig. 2.22). The major contribution is provided by aerosols: from 50 to 95% for sulfate and nitrate aerosols, from 5 to 50% for organic aerosols and soot. A pollution event is characterized by a strong increase in the aerosol contribution to b^{ext} (Table 2.13 and Figs. 2.20 and 2.21), especially for scattering.

In the framework of the North-American reglementation (*Regional Haze Rule* of the US EPA, *Environmental Protection Agency*, 2003), specific attention has been



Fig. 2.20 Visibility reduction due to particulate matter. *Left*: Rayleigh sky (17 June 2004, $\text{PM}_{10} = 20 \mu\text{g m}^{-3}$). *Right*: polluted event with high aerosol concentrations (9 June 2004, $\text{PM}_{10} = 80 \mu\text{g m}^{-3}$). PM_{10} stands for the mass of particles whose radius (in a first approximation) is less than or equal to $10 \mu\text{m}$. Credit: Airparif

Table 2.13 Comparison of the extinction coefficient for a “clean” day and a polluted day, in Los Angeles. The wavelength is in the visible region of the spectrum, $\lambda = 550$ nm. For the polluted day, the visibility reduction is related to the aerosol scattering. Source: [82]

Extinction coefficient (10^{-4} m^{-1})	“Clean” day (7 April 1983)	Polluted day (25 August 1983)
Aerosol scattering	0.26	4.08
Gas-phase scattering	0.11	0.11
NO ₂ absorption	0.01	0.03
Soot absorption	0.09	0.78
Total	0.47	5

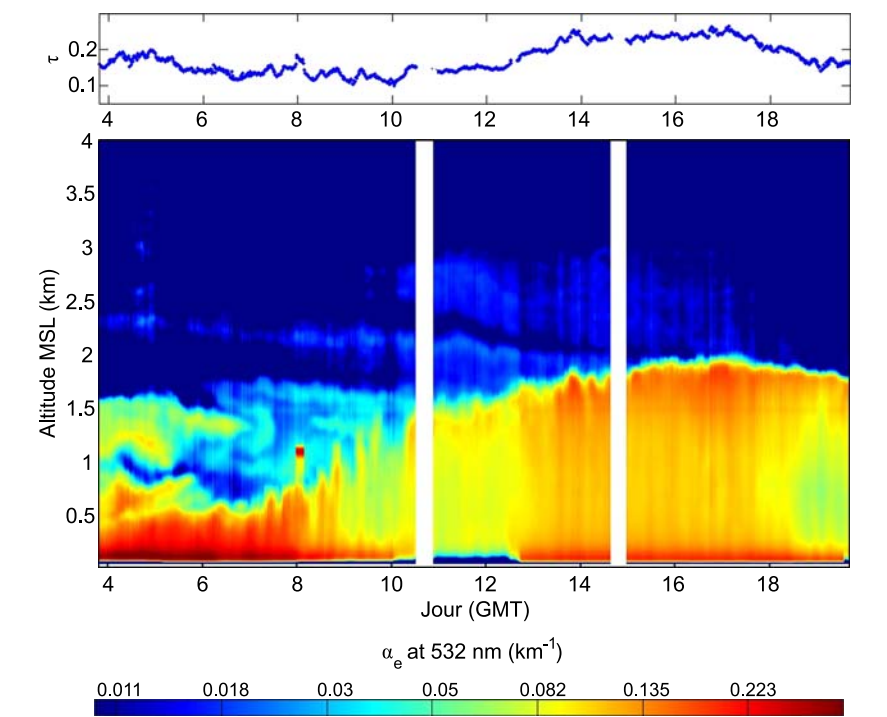


Fig. 2.21 Upper panel: evolution of the total optical depth. Lower panel: evolution of the vertical profile of the extinction coefficient, b_{ext} (here written as α_e ; in km^{-1}). The wavelength is 532 nm (visible). The observational data were measured at Paris center (“place de l’Hotel-de-Ville”, 4–18 May 2005, LISAIR campaign). Credit: Patrick Chazette, CEA

paid to visibility in the national parks. The visibility reduction is measured by the so-called *haze index*,

$$HI = 10 \ln \frac{b^{ext}}{10},$$

(2.56)



Fig. 2.22 Pollution event with high nitrogen dioxide concentrations over Paris, 1st February 2006. A maximum of about $350 \mu\text{g m}^{-3}$ was measured. Credit: Airparif ([4])

with b^{ext} the extinction coefficient. When b^{ext} is expressed as $10^{-6} \text{ m}^{-1} (\text{Mm}^{-1})$, the haze index is expressed in *deciview* (dv). Note the connection to x_v . A “clean” reference atmosphere corresponds to $b^{ext} = 10 \text{ Mm}^{-1}$. The “Rayleigh atmosphere” (namely, without any particles) is sometimes defined by $b^{ext} = 13 \text{ Mm}^{-1}$.

A few parameterizations are available for calculating b^{ext} as a function of the aerosol chemical composition, for example ([108])

$$b^{ext} = 2f(RH) \times ([(\text{NH}_4)_2\text{SO}_4] + [\text{NH}_4\text{NO}_3]) + 1.4[\text{OC}] + 10[\text{EC}] \\ + [\text{mineral}] + 0.6[\text{coarse}] + 10, \quad (2.57)$$

where $f(RH)$ is a function of the relative humidity RH (in order to describe the aerosol growth due to water condensation on nitrate and sulfate aerosols; typically, $f(\cdot)$ ranges from 2 to 3), OC stands for the organic carbon, EC for the elemental carbon, “mineral” is related to the mineral part of $\text{PM}_{2.5}$ ⁵ and “coarse” to the coarse part of the aerosol distribution (diameter above $2.5 \mu\text{m}$). In the absence of aerosols, HI is equal to 0.

As expected, the visibility strongly depends on humidity.⁶ The atmospheric dust burden is another key factor. For example, in southern Europe, the extinction coefficient may sometimes increase up to hundreds of Mm^{-1} , due to the transport of Saharian dust.

Problems Related to Chap. 2

Problem 2.1 (Radiative Forcing due to Aerosols and Direct Effect) The radiative behavior of aerosols depends not only on the size distribution but also on the chem-

⁵ $\text{PM}_{2.5}$ stands for the mass of particles whose diameter is less than or equal to $2.5 \mu\text{m}$.

⁶Think about the visibility in a fog!

ical composition (Table 2.14). This problem (taken from [58]) illustrates the sensitivity of the radiative behavior with respect to the aerosol type.

1. Estimate the *a priori* impact on the surface temperature,
 - first, of an increase in the scattering of solar radiation (sulfate aerosols),
 - and, second, of an increase in the absorption of infrared radiation (soot).

What can conclude for the mineral aerosol?
2. We use a toy model for radiative transfer. The atmosphere is supposed to be a layer of temperature T_1 . The layer does not absorb the solar radiation, absorbs the infrared radiation with an absorption coefficient f , and emits to the Earth and space a power per unit area of surface $2f\sigma T_1^4$ (half to the Earth, half to space). The Earth/atmosphere system has an albedo A with respect to the solar radiation. Motivate the expression used for the emission. Calculate the Earth's temperature as a function of F_s (solar flux), A and f . Give a coherent value for f so that $T_0 = 288$ K.
 Data: $A = 0.3$; $\sigma = 5.67 \times 10^{-8} \text{ W m}^{-2} \text{ K}^{-4}$; $F_s = 342 \text{ W m}^{-2}$.
3. Consider the variations δT_0 due to the modifications of the radiative properties of the atmospheric layer (δf and δA). To which aerosols are associated variations $\delta f > 0$ and $\delta A > 0$?
 Express δT_0 as a function of δf and δA (use the logarithmic derivative: $d(\ln x) = dx/x$). Prove that there exists a critical value of $\delta A/\delta f$.

Three-dimensional simulations illustrate the uncertainties of the radiative impact due to mineral aerosols. The negative radiative forcing in the shortwave radiations is likely to have the same magnitude as the positive radiative forcing in the longwave radiations. The resulting total contribution is estimated to be $[-0.6, +0.4] \text{ W m}^{-2}$ ([106], see the reference below). This means that the sign of the radiative forcing is not known, even if it is likely to be negative.

See also Problem 2.3 for another viewpoint.

Solution:

1. An increase in the scattering of the solar radiation leads to an increase in the albedo of the Earth/atmosphere system, namely to a cooling. An increase in the absorption of the infrared radiation is similar to an increase in the greenhouse effect and should result in an increasing temperature.
 Soot has an effect similar to a greenhouse gas, on the contrary to sulfate aerosols. We cannot conclude for mineral aerosols.
2. The emitted fraction corresponds to the absorbed fraction, which motivates the use of f for emission. At the radiative equilibrium for the Earth/atmosphere system,

$$(1 - A)F_s = f\sigma T_1^4 + (1 - f)\sigma T_0^4, \quad 2f\sigma T_1^4 = f\sigma T_0^4,$$

Table 2.14 Radiative properties of aerosols with respect to the solar and infrared radiation

Aerosol type	Solar radiation	Infrared radiation
Sulfate	scattering	–
Soot	absorption	absorption
Mineral	scattering	absorption

thus

$$\left(1 - \frac{f}{2}\right) \sigma T_0^4 = (1 - A) F_s.$$

In order to have $T_0 = 288$ K (mean surface temperature), we take $f \simeq 0.78$.

3. $\delta f > 0$ corresponds to the case of soot; $\delta A > 0$ corresponds to the case of sulfate aerosols. The mineral aerosols are associated to both variations.

Taking the logarithmic derivative of the previous equation yields

$$4 \frac{\delta T_0}{T_0} = \frac{\delta f}{2(1 - \frac{f}{2})} - \frac{\delta A}{1 - A}.$$

In order to assess the sign of δT_0 , there exists a critical value

$$\frac{\delta f}{\delta A} = \frac{2(1 - \frac{f}{2})}{1 - A}.$$

To know more ([106]):

I.P. ON CLIMATE CHANGE, *Climate Change 2001. IPCC Third Assessment Report. The Scientific Basis*, 2001. WMO and UNEP (Chap. 6, pp. 372–373)

Problem 2.2 (Cloud Albedo and Twomey Effect) This problem aims at calculating the cloud albedo in the visible region of the electromagnetic spectrum.

Consider a cloud with thickness h and with a liquid water content L (defined as the mass of liquid water per air volume). The cloud is composed of water drops with a number density n , supposed to have the same *effective* radius (r_e). The effective radius is computed as a mean radius weighted by the drop cross sections (that play a leading role for the radiative properties).

1. Calculate the cloud optical depth τ_c in the visible region. Give two formulations: the first one as a function of the drop number density n , the second one as a function of the effective radius r_e . Let ρ_w be the water density.
2. The observational data indicate that the cloud effective radius ranges from 5 to 8 μm over urban (polluted) areas, from 8 to 10 μm over remote continental regions, and from 10 to 15 μm over oceans. Investigate the impact of a division by two on the effective radius for the drop number density, the drop surface and the optical depth.
3. The cloud albedo can be parameterized as a function of the optical depth, as

$$A_c = \frac{\tau_c}{\tau_c + 7.7}.$$

Plot the evolution of A_c as a function of the cloud microphysical properties. Compare the cloud albedo in a marine environment ($n \simeq 100 \text{ cm}^{-3}$) and in a polluted area ($n \simeq 1000 \text{ cm}^{-3}$).

Data: $L = 0.5 \text{ g m}^{-3}$ and $h = 100 \text{ m}$.

Solution:

1. Assuming that the cloud is homogeneous, $\tau_c = b^{ext} \times h$ (we omit the dependence with respect to the wavelength in the notations). We use $b^{ext} = \pi r_e^2 Q^{ext} n$, with $Q^{ext} \simeq 2$ (Sect. 2.1.7). Thus

$$\tau_c = 2\pi r_e^2 n h.$$

The use of the liquid water content, L , leads to the elimination of n or of r_e since

$$L = \frac{4}{3} \pi r_e^3 \times n \times \rho_w.$$

We obtain the possible expressions, as a function of the radius,

$$\tau_c = \frac{3}{2} \frac{L h}{r_e \rho_w},$$

or as a function of the drop number density,

$$\tau_c = h \left(\frac{9}{2} \frac{n \pi L^2}{\rho_w^2} \right)^{1/3}.$$

The optical depth is therefore an increasing function of the drop number density and a decreasing function of the drop radius.

2. Dividing by 2 the effective radius implies a multiplication by 8 of n (number density). The total surface and the optical depth are proportional to $n r^2$ and, hence, are multiplied by 2.
3. The cloud albedo is an increasing function of the optical depth. The sensitivity with respect to the microphysical properties is then similar to that of the optical depth.

We refer to Fig. 2.19. The albedo for a marine cloud is about 0.45; it is about 0.63 for a cloud in an urban area.

Problem 2.3 (Albedo of an Aerosol Layer) This problem, partially taken from [130], is the follower of Problem 2.1. We want to investigate the impact of the size distribution.

Consider an aerosol layer defined by its optical depth τ and its scattering albedo ω_d . Let β be the fraction of the scattered solar radiation that is reflected back to space. Moreover, the radiation transmitted by the layer is supposed to reach directly the Earth's surface, on which it is reflected with an albedo A_s .

1. Evaluate the fraction r of the incident radiation that is directly reflected back to space. Let t be the transmitted fraction. We do not take into account the contributions due to the reflection at ground.
2. Calculate ΔA the modification, due to the aerosol layer, of the albedo for the Earth/atmosphere system. Hint: take into account the multiple reflections between the Earth's surface and the aerosol layer.
3. The impact of the aerosol layer on the global albedo depends on the competition between scattering and absorption (both define extinction). Show that there exists a critical value ω_d that determines the transition from a cooling effect to a warming effect. Use asymptotic expansions with respect to τ (its value is about 0.1).

4. Show that a non-absorbing aerosol layer has always, as expected, a cooling effect. This is typically the case of sulfate aerosols.
5. We consider the visible radiation ($\lambda = 550 \text{ nm}$). For a mineral aerosol, ω_d is a decreasing function of the diameter (d_p). Its value is about 0.96 for $d_p = 0.2 \mu\text{m}$ and 0.72 for $d_p = 8 \mu\text{m}$. Estimate the resulting impact.

Data: surface albedo $A_s = 0.15$, $\beta \simeq 0.5$ for fine aerosols ($d_p \simeq 100 \text{ nm}$), $\beta \simeq 0.2$ for coarse aerosols ($d_p > 1 \mu\text{m}$).

Solution:

1. The incident radiation has a *direct* transmitted fraction ($\exp(-\tau)$) and a fraction subject to extinction ($1 - \exp(-\tau)$).

For the extinction, a fraction ω_d is scattered while a fraction $(1 - \omega_d)$ is absorbed.

A fraction β of the scattered fraction is reflected back to space. A fraction $(1 - \beta)$ is transmitted to the Earth's surface upon scattering, and has to be added to the direct transmitted fraction.

Finally, we obtain

$$r = \beta\omega_d(1 - \exp(-\tau)), \quad t = \exp(-\tau) + (1 - \beta)\omega_d(1 - \exp(-\tau)).$$

2. Let t_n be the fraction of the radiation that is transmitted to the Earth's surface after n "interactions" with the aerosol layer. After a reflection on the Earth's surface, the fraction becomes $A_s \times t_n$. After a new interaction with the aerosol layer, a fraction t is transmitted to space (to be taken into account in the global albedo) while a fraction r is reflected to the ground. Therefore, the iteration reads

$$t_{n+1} = r \times A_s \times t_n, \quad r_{n+1} = t \times A_s \times t_n,$$

and finally $t_n = (r A_s)^{n-1} t$, $r_n = t A_s (r A_s)^{n-1} t$. The total reflected fraction is

$$A_a = r + \sum_{n=1}^{\infty} r_n = r + \frac{t^2 A_s}{1 - r A_s}.$$

The albedo variation is $\Delta A = A_a - A_s$.

3. The aerosol albedo has a cooling effect or a warming effect, depending on the sign of ΔA : for example, if $\Delta A > 0$, there is an increase in the global albedo, which results in a cooling.

Using the asymptotic expansions $r \simeq \beta\omega_d\tau$ and $t \simeq 1 - \tau + (1 - \beta)\omega_d\tau$, up to second order in τ , we get

$$\Delta A = [\omega_d(\beta(1 - A_s)^2 + 2A_s) - 2A_s]\tau.$$

The critical value is then

$$\omega_d^* = \frac{2A_s}{\beta(1 - A_s)^2 + 2A_s}.$$

If $\omega_d > \omega_d^*$, $\Delta A > 0$ (cooling effect). Note that a cooling effect is expected for high values of ω_d (scattering is dominant with respect to absorption). Moreover, the critical value is a decreasing function of β (increasing the fraction scattered back to space favors the cooling effect).

With the numerical data, we calculate for coarse aerosols ($\beta \simeq 0.2$), $\omega_d^* \simeq 0.67$, and for fine aerosols ($\beta \simeq 0.5$), $\omega_d^* \simeq 0.45$.

4. For a non-absorbing layer (the extinction is only composed of scattering: $\omega_d = 1$), we obtain

$$\Delta A = \beta(1 - A_s)^2 \tau > 0.$$

The effect is a cooling effect, as expected.

5. The values of ω_d are much greater than the critical value. The impact is a cooling effect in the visible region and a warming effect in the infrared region.

To know more ([24, 99]):

S. NEMESURE, R. WAGENER, AND S. SCHWARTZ, *Direct shortwave forcing of climate by the anthropogenic sulfate aerosol: sensitivity to particle size, composition, and relative humidity*, J. Geophys. Res., **100** (1995), pp. 26105–26116 (for the sulfate aerosols)

R. CHARLSON, J. LANGNER, H. RODHE, C. LEOVY, AND S. WARREN, *Perturbation of the northern hemisphere radiative balance by backscattering from anthropogenic sulfate aerosols*, Tellus, **43AB** (1991), pp. 152–163

Problem 2.4 (Nuclear Winter) In 1982, Crutzen and Birks ([27]) described the impact of a nuclear war: it would lead to a strong global cooling, which was referred to as *nuclear winter*. The context was the “Cold War” between the USA and the USSR, with the peak of the so-called “Euromissile crisis” (early 1980s). In the 1980s, many studies, based on the use of climate models, have confirmed this preliminary study.

More attention has been recently paid to this subject due to the possibility of a *regional* nuclear conflict.

Describe the processes that could explain the cooling effect. Comment on the long-term impact (more than ten years), as compared to the impact of volcanic eruptions (a few years, Exercise 2.9).

Data ([121]):

- emissions of smoke and ashes after the explosions: 150 Tg;
- stratospheric residence time of smoke and ashes: 5 years;
- radiative forcing for the solar radiation averaged over one decade (after ten years): -100 W m^{-2} (-20 W m^{-2});
- ΔT at the Earth’s surface during one decade (after ten years): -7 K (-4 K);
- precipitations: -50% .

Solution:

A huge amount of smoke and ashes (particles) would be injected into the atmosphere, just after the explosion. The negative radiative forcing in the shortwave radiation is similar to that of the sulfate aerosols.

The high temperatures following the explosions would favor direct injection into the upper stratosphere (*lofting*), while the sulfate aerosols are rather near the tropopause. This results in a higher residence time and then a longer impact (more than one decade).

To know more ([27, 121]):

P. CRUTZEN AND J. BIRKS, *The atmosphere after a nuclear war. Twilight at noon*, Ambio, **11** (1982), pp. 114–125

A. ROBOCK, L. OMAN, AND G. STENCHIKOV, *Nuclear winter revisited with a modern climate model and current nuclear arsenals: still catastrophic consequences*, J. Geophys. Res., **112** (2007), p. 13107



<http://www.springer.com/978-90-481-2969-0>

Fundamentals in Air Pollution

From Processes to Modelling

Sportisse, B.

2010, X, 299 p., Hardcover

ISBN: 978-90-481-2969-0